

1 **Temperature-related developmental plasticity, not selection, affects**
2 **offspring body size and shape in a bird of prey**

3
4 Running title: Antagonistic effects of temperature on body morphology

5
6 Alejandro Corregidor-Castro^{1,2*}, Andrea Romano³, Michael Butler-Margalef⁴, Jacopo G.
7 Cecere⁵, Jennifer Morinay^{5,6}, Michelangelo Morganti^{2,7}, Diego Rubolini^{3,7}, Andrea Pilastro^{1,2}

8 ¹ *Dipartimento di Biologia, Università di Padova, Via U. Bassi 58/B, I-35131 Padova, Italy*

9 ² *National Biodiversity Future Centre, Piazza Marina 61, 90133, Palermo, Italy*

10 ³ *Dipartimento di Scienze e Politiche Ambientali, Università degli Studi di Milano, via Celoria 26, I-20133 Milano,*
11 *Italy*

12 ⁴ *GRECO, Institute of Aquatic Ecology, University of Girona, Girona, Spain*

13 ⁵ *Area Avifauna Migratrice, Istituto Superiore per la Protezione e la Ricerca Ambientale (ISPRA), via Ca'*
14 *Fornacetta 9, I-40064 Ozzano Emilia (BO), Italy*

15 ⁶ *Ecology & Evolutionary Biology, School of Biosciences, University of Sheffield, Sheffield S10 2TN, UK*

16 ⁷ *Consiglio Nazionale delle Ricerche – Istituto di Ricerca sulle Acque (CNR-IRSA), Via del Mulino 19, I-20861*
17 *Brugherio, Italy*

18
19 *Corresponding author

20 Email: alejandro.corregidorcastro@unipd.it

21
22 A.CC.: <https://orcid.org/0000-0002-7666-2153>

23 A.R.: <https://orcid.org/0000-0002-0945-6018>

24 M. BM.: <https://orcid.org/0009-0004-4524-3062>

25 J.G.C.: <https://orcid.org/0000-0002-4925-2730>

26 J.M.: <https://orcid.org/0000-0002-7905-9691>

27 M.M.: <https://orcid.org/0000-0002-8047-0429>

28 D.R.: <https://orcid.org/0000-0003-2703-5783>

29 A.P.: <https://orcid.org/0000-0001-9803-6308>

30

31

32 **Abstract**

33 Recent climate warming has led to a reduction in bird body size and a relative elongation of their
34 appendages, consistent with Bergmann's and Allen's ecogeographical rules. These changes are
35 generally interpreted as thermoregulatory adaptations for more efficient passive heat dissipation;
36 however, direct evidence supporting this assumption is currently missing, and laboratory studies
37 failed to find significant thermoregulatory benefits associated with body size or appendage
38 length. To test whether body shrinking and shape-shifting provide a fitness advantage under
39 climate warming, we experimentally altered nest temperatures in a lesser kestrel (*Falco*
40 *naumanni*) population exposed to high temperatures during the nestling stage. We found that nest
41 temperature was associated with nestling mortality. Among nestlings that survived to fledging,
42 temperature was negatively correlated with their near-fledging body size (mass and tarsus length)
43 and positively correlated with their relative bill length. Contrary to the thermoregulation
44 hypothesis, we found that nestlings that were larger at hatching had higher survival, irrespective
45 of the nest temperature, whereas relative bill length did not confer any significant survival
46 advantage. Collectively, our findings suggest that temperature-related developmental plasticity,
47 rather than selection, is a key driver of observed morphological changes in natural bird
48 populations, and that these changes are not adaptive.

49

50 **Keywords:** Allen's rule, Bergmann's rule, bill length, body size, nest temperature, heatwaves

51

52 **Introduction**

53 Global climate has experienced significant warming in recent decades, accompanied by more
54 frequent and intense temperature extremes (Lee et al., 2023). During this period, evidence has
55 accumulated that many homeothermic animals, including birds, have progressively decreased in
56 size and increased the relative length of their appendages, associated with rising temperatures
57 (Gardner et al., 2011; Campbell-Tennant et al., 2015; van Gils et al., 2016; Prokosch et al., 2019;
58 Tian and Benton, 2020; Ryding et al., 2021; Dubiner and Meiri, 2022; Youngflesh et al., 2022;
59 Zimova et al., 2023; Romano et al., 2024). These morphological shifts align with Bergmann's
60 and Allen's ecogeographical rules, which posit that animals in warmer climates—typically lower
61 latitudes and altitudes—tend to have smaller body sizes and relatively longer appendages than
62 those in colder environments (Bergmann, 1847; Allen, 1877). Smaller body size and longer
63 appendages increase the surface-to-volume ratio, enhancing passive heat dissipation in hot
64 climates, while lower surface-to-volume ratios are advantageous in colder climates (Mayr, 1956).
65 Although the extent of changes in body size and appendage length (e.g., bill length; Tattersall et
66 al., 2017) varies among species (Ryding et al., 2024; Santoro and Calzada 2022), there is
67 extensive empirical support for a widespread avian response to warming temperatures (e.g.,
68 Campbell-Tennant et al., 2015; Gardner et al., 2016; van Gils et al., 2016; Weeks et al., 2020;
69 Jirinec et al., 2021; Romano et al., 2024). However, the underlying mechanisms driving these
70 rapid changes remain uncertain.

71 Two non-mutually exclusive explanations have been proposed to explain the observed
72 rapid shifts in body size and relative appendage length among bird populations in response to
73 climate warming (Campbell-Tennant et al., 2015; Cardilini et al., 2016; Youngflesh et al., 2022;
74 Fröhlich et al., 2023). The first hypothesis suggests that these phenotypic shifts may be adaptive
75 evolutionary responses to selection for enhanced heat dissipation capability, conferred by a
76 higher surface-to-volume ratio (Ryding et al., 2021; Youngflesh et al., 2022). For example,
77 relatively longer bills may offer a thermoregulatory advantage in warming climates because their
78 vascularization improves dry heat dissipation (Tattersall et al., 2017; Schraft et al., 2019).
79 Similarly, other non-feathered appendages, such as the tarsus, may enhance heat dissipation
80 during heat stress in certain species (McQueen et al., 2022). Thus, individuals with smaller
81 bodies and relatively larger appendages might increase their efficiency in dry heat dissipation,
82 reducing the costs associated with active evaporative cooling (Greenberg et al., 2012; Song and

83 Beissinger, 2020). The strongest shifts in body size and shape have been observed in populations
84 exposed to more intense climate warming, supporting the adaptive hypothesis for increased
85 surface-to-mass ratios (Youngflesh et al., 2022; Dubiner et al., 2022; Romano et al., 2024).
86 However, direct evidence showing that individuals with smaller size and a higher surface-to-
87 volume ratio have increased fitness under naturally high temperatures is still lacking (Siepielski
88 et al., 2019; Nord et al., 2024).

89 The second hypothesis arises from observations that in several studies, avian nestlings
90 exposed to high temperatures during development show reduced growth rates (James, 1991;
91 Burness et al., 2013; Andrew et al., 2017; Larson et al., 2018; Corregidor-Castro and Jones,
92 2021; Weeks et al., 2022; Shipley et al., 2022) and relatively longer bills by fledging (Tabh et al.,
93 2024). It has been suggested that climate-related shifts in body size and shape observed in recent
94 cross-sectional studies on bird populations may result from developmental plasticity rather than
95 selection (James, 1991; Tabh and Nord, 2023). Experiments in which developmental temperature
96 was experimentally controlled – either in the lab (e.g., Burness et al., 2013; Tabh et al., 2024;
97 Shipley et al., 2022) or under natural conditions (Sauve et al., 2021) – provided partial support
98 for the developmental hypothesis, possibly because the effect of temperature on bird growth may
99 depend on whether it is experimentally raised above or lowered below the optimal range for
100 nestling development (Shipley et al., 2022; Tabh and Nord, 2023; Nord et al., 2024).
101 Importantly, temperature-related developmental plasticity has shown minor effects on
102 thermoregulation, survival, and reproduction under laboratory conditions (Tabh and Nord, 2023;
103 Hope and Angelier, 2024).

104 While both selection and plasticity hypotheses are plausible and may operate
105 simultaneously, whether body size and shape shifting observed in natural populations is the
106 consequence of a thermoregulatory advantage remains an area of ongoing debate (Nord et al.,
107 2024; Youngflesh et al., 2024). Clarifying the roles of these mechanisms is crucial, as these
108 changes could signify rapid adaptation to climate warming or serve as early indicators of
109 potential population decline (Cerini et al., 2023). To address these gaps, we conducted a nest
110 temperature manipulation experiment in a Mediterranean population of the cavity-nesting lesser
111 kestrel (*Falco naumanni*), a small (140 g) bird of prey. Lesser kestrels readily breed in nest
112 boxes and experience high temperatures during the breeding season, which has adverse effects
113 on nestling survival (Catry et al., 2011; Catry et al., 2015; Campobello et al., 2017). Nest

114 temperature was experimentally reduced in a group of nest boxes by shading them from direct
115 sunlight, a manipulation that reduces internal nest temperatures by approximately 4°C as
116 compared to unshaded, control boxes and increase nestling survival and growth (Corregidor-
117 Castro et al., 2023). Here, we expand on this approach to address two questions. First, we tested
118 whether nest temperature affects nestling body size and bill length near fledging. Bill is
119 considered an important heat dissipation organ in birds (Tattersall et al., 2017). Second, given
120 that high nest temperature is linked to significant nestling mortality (Corregidor-Castro et al.,
121 2023), we examined whether body morphology during early development is differently
122 associated with subsequent survival to fledging in the two experimental groups. If smaller body
123 size and relatively longer appendages confer a thermoregulatory advantage, positive selection for
124 nestling body size, that it is typically observed in birds (Krist, 2011), should be weaker or even
125 negative in control nests as compared to shaded ones (Siepielski et al., 2019).

126

127 **Material and Methods**

128 *Study species, study area and general field procedures*

129 Our experiment was conducted in the city of Matera, southern Italy (40°66'N, 16°61'E), home to
130 a large population of lesser kestrels with approximately 1,000 breeding pairs (La Gioia, 2017).
131 These kestrels nest in building cavities and artificial nest boxes (Morinay et al., 2021). Clutch
132 size ranges from 3 to 5 eggs, which are laid from late April to early May (Ramellini et al., 2022).
133 Both parents incubate the eggs for around 31 days and continue feeding the young for about 40
134 days after hatching (Podofillini et al., 2018).

135 The study took place over two breeding seasons (May – July 2021 and 2022) on a large
136 roof (600 m²), where 66 nest boxes were installed between 2008 and 2010. These nest boxes
137 have been consistently occupied by lesser kestrels (Corregidor-Castro et al. 2023). From the start
138 of each breeding season, we monitored nest boxes every 3-4 days to record laying and hatching
139 dates, and both clutch and brood size, until nestlings were approx. 15 days old, after which visits
140 ceased to minimize the risk of premature fledging (Podofillini et al., 2018). Upon hatching,
141 individual nestlings were temporarily marked with unique dot patterns on the head and later
142 ringed at around 10 days of age. Nestlings were ranked by hatching order, with rank 1 assigned

143 to the first-hatched nestling. Nestlings were blood-sampled and sexed using standard molecular
144 markers (Corregidor-Castro et al. 2023).

145

146 *Nest temperature manipulation*

147 We performed an experimental manipulation of the nest boxes to partially decouple external
148 environmental temperature (recorded at the Matera city meteorological station, see Corregidor-
149 Castro et al. (2023)) from the temperature recorded inside the nest. To do so, upon hatching, we
150 created temporally matched groups (hereafter “synchronous groups”) of at least two nest boxes,
151 paired based on hatching date, clutch size, and other nest characteristics such as orientation and
152 sun exposure. Within each synchronous group, one randomly chosen nest box was covered on
153 the top and sides with a 0.5 cm thick plank of plywood, forming an open box structure (41 × 36
154 × 45 cm; shaded nest box). The other nest box in the group was left unmanipulated (control nest
155 box). We recorded nest box internal temperature using temperature loggers (Elitech RC-5+,
156 Elitech, UK; accuracy 0.5°C) attached to the internal side of the wooden back panel of each nest
157 box. To protect the panel from direct sunlight, a 40 × 40 cm tile was placed outside on the back
158 of each nest box, shading the wall while allowing air to circulate. Temperature loggers were set
159 to record every 15 min, from hatching of the first nestling until the end of the monitoring season,
160 when they were retrieved. All loggers were certified as being individually calibrated by the
161 supplier. Preliminary testing in a thermostatic chamber at constant temperature for 12 hours
162 confirmed negligible differences between loggers.

163 To test the effect of nest temperature on nestling body size and shape near fledging, we
164 calculated the mean of the maximum daily temperatures recorded in each nest box over the 10
165 days prior to the last nestling measurement (hereafter T_{nest}). This period corresponded to the
166 minimum interval between the start of the experimental manipulation and the age when nestlings
167 were last measured, excluding the setup day and the final measurement day. We used maximum
168 daily temperatures because previous studies demonstrated that lesser kestrel nestlings are
169 sensitive to high nest temperatures, which are associated with reduced survival and growth
170 (Catry et al. 2015; Corregidor-Castro et al. 2023).

171

172 *Nestling morphology*

173 We obtained morphological measurements of nestlings during three monitoring visits. In the first
174 visit (hereafter at-hatching), when nestlings were approximately 1 day old (± 1 day), we recorded
175 body mass, using an electronic scale (accuracy 0.1 g), and tarsus length, using a calliper
176 (accuracy 0.1 mm). To minimize disturbance during this sensitive stage, bill length was not
177 measured at this time. In total, we measured body mass in 185 nestlings (control = 88; shaded =
178 97; 73 broods) and tarsus length in 196 nestlings (control = 93; shaded = 103; 76 broods). This
179 visit marked the start of the experimental treatment.

180 Three days later, when nestlings were approximately 4 days old (± 1 day), we obtained a
181 second set of measurements (hereafter near-hatching) for body mass and tarsus length (n = 182
182 nestlings: control = 85, shaded = 97; 74 broods) and the first measure of bill length (n = 179
183 nestlings: control = 82, shaded = 97; 73 broods). Bill length was measured as the distance from
184 cere to bill tip using a caliper. These measurements allowed us to calculate early growth rates in
185 body size, based on the daily increase in body mass and tarsus length from age 1 (at hatching) to
186 age 4 (at near-hatching). By this time, nestlings had already been exposed to the experimental
187 treatment, but no significant differences in morphology or mortality were detected between
188 control and shaded groups (see Table S1). We limited our estimation of body growth to this
189 initial period of development to minimize temperature-related differences in mortality and
190 growth rate between control and shaded nestlings.

191 A final measurement visit was conducted when nestlings were on average 15.6 ± 1.7 days
192 old (range 13–20 days, hereafter near-fledging). This age corresponded with the end of the linear
193 growth phase (Romano et al., 2021) and is expected to predict body size at fledging (see
194 Braziotis et al. 2017). We did not measure older nestlings for two reasons. First, since nestlings
195 start to spend significant amount of time outside the nest after this age (Corregidor-Castro et al.,
196 2024), their morphological measurements could not be related to nest manipulation and
197 temperature. Second, capturing near-fledging individuals may have increased the risk of
198 premature abandoning of the colony roof (Podofillini et al., 2018). Due to mortality between
199 visits, sample size for this final visit was reduced to 147 nestlings (control = 49, shaded = 98; 55
200 broods). To assess fledging survival, we conducted a final check when nestlings were
201 approximately 25 days old. Although lesser kestrel juveniles leave the colony roof at around 37

202 days of age, mortality between age 25 and 37 days is virtually absent (A. Corregidor-Castro,
203 personal observations). Any nestling missing from the colony roof by age 25 days was therefore
204 assumed to be dead, although the exact cause and date of death was occasionally unknown
205 (Corregidor-Castro et al., 2023), and thus nestlings that were alive at age 25 days were
206 considered to have successfully fledge from the colony.

207 Passive heat dissipation through the bill is expected to depend on bill surface and
208 therefore bill area should reflect dry heat dissipation capability more closely than bill length
209 (Tattersall et al., 2017). However, measuring bill area is a lengthy procedure which would have
210 unduly prolonged researchers' visits at the colony and increased disturbance. In a separate
211 sample of 26 nestlings (in 2021), we verified this proxy by correlating bill length (cere-to-tip
212 distance) with bill surface area, obtained from digital photos taken of the left side of the head on
213 a standardized support with a reference scale (see Fig. S1a), followed by a second photo to
214 estimate a measurement of repeatability. Bill lateral area was calculated using ImageJ, blind of
215 the nestling identity (Schneider et al., 2012; Fig. S1b). Nestling bill length was also measured
216 twice following a blind procedure (i.e. one operator placed the calliper and the measure was read
217 and transcribed by a second operator). The measurements were highly repeatable (bill length,
218 repeatability = 0.93 ± 0.02 ; bill lateral area, repeatability = 0.99 ± 0.01 ; Lessells and Boag, 1987)
219 and we therefore used the average of the two measurements. Upper mandible area (lateral area \times
220 2) and bill length were significantly correlated ($r = 0.87$, $p < 0.001$, $n = 26$), supporting bill
221 length as a reliable proxy for bill area.

222

223 *Statistical analyses*

224 **Effect of shading on nest temperature** - To test if shading effectively reduced T_{nest} , we used a
225 linear mixed model (LMM) where T_{nest} was the response variable, with year and experimental
226 treatment as two-level fixed factors (year: 2021, 2022; shading: control, shaded). To account for
227 seasonal variation and to align with the pairwise nature of the experimental design, we included
228 synchronous group identity as a random intercept effect (here and in all subsequent models).

229

230 **Effect of shading on nestling size and shape near fledging** – We examined the effect of
231 shading on nestling morphology near fledging (body mass, tarsus length, and bill length) by
232 fitting three separate LMMs, each with one morphological trait as the response variable. In each
233 model, experimental treatment was included as a fixed factor, along with year, brood size, age
234 and hatching rank of the nestling, as they could influence nestlings' final size (Aparicio, 1997;
235 Braziotis et al. 2017; Podofillini et al. 2019). Furthermore, we included the sex of the nestling (0
236 = female, 1 = male) to account for sex-linked size differences. We included nest identity as a
237 random factor to control for the non-independence of nestlings from the same brood, along with
238 synchronous group identity. Considering that some of the nests of the two experimental groups
239 had similar nest temperatures (caused by the variation in the external temperatures and the
240 asynchrony between nests; Fig S2), we fitted three additional models using T_{nest} as a covariate,
241 instead of the experimental treatment. If temperature differences are the primary driver of any
242 morphological differences between experimental groups, we expected a stronger statistical effect
243 of T_{nest} than experimental treatment.

244 To further investigate the relationship between temperature and relative bill length
245 (accounting for body size), we included body mass and tarsus length as covariates in a model
246 with bill length as the response variable. Fixed and random effects were as above, and an
247 alternative model with T_{nest} instead of the experimental treatment as a covariate was also fitted.
248 Because tarsi are naked appendages and can be related to heat dissipation (Ryeland et al., 2019;
249 McQueen et al., 2023) we fitted two additional models with tarsus length as the response
250 variable and body mass as a covariate, one including the experimental treatment and the other the
251 T_{nest} as predictors. These models contained the same predictors as those stated above.

252 Finally, given the positive correlation between body mass, tarsus length, and bill length,
253 we conducted a Principal Component Analysis (PCA) of these traits to generate independent
254 indices of body size and shape. In particular, the first axis (PC1) represents a metric of body size
255 variation (Weeks et al., 2020), while the second axis (PC2) should be regarded as a metric of the
256 variation in the three body measures removing differences in size (see a similar approach to the
257 analysis of bill size and shape in Darwin finches, Grant and Grant, 2008). We used the resulting
258 PCA scores to fit two LMMs with the experimental treatment and nestling sex as fixed factors,
259 and year, brood size, age, and hatching rank as covariates. These models were also repeated with

260 T_{nest} as a covariate instead of the experimental treatment to further analyze the impact of
261 temperature on nestling morphology.

262

263 **Effect of nestling size and early development on subsequent survival** – We first tested
264 whether nestlings from the two experimental groups differed in any relevant parameter at
265 hatching (age 1) and at near-hatching (age 4). For age 1, we used LMMs to analyze differences
266 in body mass, tarsus length, age of the nestling and brood size, with each variable included as a
267 response variable. The experimental treatment was set as a fixed factor, with nest and
268 synchronous group identity as random intercepts to account for group effects. For age 4, we
269 applied similar LMMs for the same variates measured in the previous visit, with the addition of
270 bill length (first measured at age 4) and its relative size compared to body size. Two additional
271 LMMs tested whether growth rates in body mass and tarsus length differed between ages 1 and
272 4. We also evaluated differences in survival from age 1 to age 4 using a binomial generalized
273 linear mixed model (GLMM) with a logit link function. No significant differences were found
274 between shaded and control nestlings for any trait (see Table S1).

275 Given that nestlings measured at age 1 and age 4 varied in age (0-2 days for nestlings
276 measured at hatching, and 3-5 days for nestlings measured at near-hatching), and that these age
277 differences impacted all morphological measurements, we calculated age-corrected values for
278 body mass and tarsus length (for both ages) and bill length (for age 4 only). These values were
279 generated as standardized residuals from a model with age as a fixed factor (Salas et al., 2022).
280 Next, we analyzed survival as a function of age-corrected body mass and tarsus length at
281 hatching using a GLMM with binomial error distribution and logit link. Survival (0 = did not
282 survive; 1 = survived) was set as the dependent variable, with the experimental treatment, age-
283 corrected body size measurements (mass or tarsus length), and their interaction as fixed factors.
284 A significant interaction between nestling morphology and shading would indicate that nest
285 temperature affects selection strength and/or direction on body size and morphology. As above,
286 we included sex, nestling rank, and brood size as fixed factors to account for their effects on
287 survival. We repeated these analyses for age 4 nestlings, including age-corrected bill and relative
288 bill length. Finally, we used a principal component analysis (PCA) on body mass, tarsus length,
289 and bill length data from age 4 to derive an overall body size (PC1) and body shape index (PC2).

290 Using GLMMs similar to the previous analyses, we tested whether survival to fledging depended
291 on nestling body size (PC1) and body shape (PC2).

292

293 **Effect of nestling early growth on subsequent survival** – We examined whether nestlings’
294 early growth rate, calculated as the daily difference in age-corrected body mass and tarsus length
295 between ages 1 and 4, was associated with subsequent survival to fledging, and whether this
296 association differed between the two experimental treatments. We used GLMMs, with individual
297 survival as the binomial response variable, and the experimental treatment, growth rate (in body
298 mass or tarsus length), and their interaction as fixed factors. We included sex, nestling rank, and
299 brood size as fixed factors to control for their potential effects on survival.

300

301 All statistical analyses were carried using the statistical software R, version 4.3.3 (R Core Team,
302 2024). We fitted LMMs and binomial GLMMs using the “lme4” and “glmmTMB” libraries
303 (Bates et al., 2015; Brooks et al., 2017). We checked for collinearity and inspected residual
304 diagnostics using the “performance” package (Lüdtke et al., 2021). In all our mixed models, we
305 mean-centred the predictors. Significance of fixed predictors in LMMs and GLMMs were
306 assessed by likelihood ratio tests (Singmann et al., 2015). For clarity in the text, we present the
307 models including only significant predictors, where full models (with non-significant predictors)
308 are given in the supplementary material (Tables S2-S12). In survival analyses, we retained the
309 interaction between nestling morphology and the experimental treatment even when non-
310 significant, to formally test if selection on morphology was influenced by nest temperature. In all
311 survival models, nestling morphology significantly predicted survival even after excluding non-
312 significant interactions (results not shown). Means and parameter estimates are provided with
313 standard errors, unless noted otherwise.

314

315 **Results**

316 *Effect of shading on nest temperature*

317 Shading reduced nest temperatures during nestling growth. In particular, recorded nest
318 temperatures (T_{nest}) were significantly higher in control nest boxes compared to shaded ones

319 (control: $41.9 \pm 0.3^\circ\text{C}$; shaded: $39.1 \pm 0.2^\circ\text{C}$; $F_{2,52} = 54.6$; $p < 0.001$), although temperatures
320 largely overlapped between the two experimental groups (Fig. S2a). This resulted from nest
321 temperature depending not only on our shading manipulation but also on occurrences of hot
322 weather peaks during the breeding season and the differences in nest phenology (Fig. S2b).

323

324 *Effect of shading on nestling size and shape near fledging*

325 Control nestlings had lower body mass and shorter tarsus length near fledging compared to their
326 shaded counterparts, indicating high maximum temperatures depressed nestling growth (Table
327 1a,b; Fig. 1). This conclusion was further supported by a qualitatively similar but stronger
328 negative effect of the actual nest temperatures experienced by nestlings (T_{nest}) on nestling size
329 (Table S3a,b). In contrast, we found no significant effect of either experimental treatment or T_{nest}
330 on nestling bill length (Table 1c; Fig. 1; Table S3c). However, when statistically controlling for
331 body size, bill length was positively correlated with T_{nest} . The experimental treatment effect on
332 relative bill length followed the same positive direction, although not statistically significant
333 (Table S4). Relative tarsus length showed no correlation with either the experimental treatment
334 or T_{nest} (Table S5).

335 Similar results were obtained using principal component analysis (PCA) to describe
336 variation in nestling morphology. PC1, accounting for 78% of variance, was positively loaded on
337 body mass, tarsus length and bill length, representing an overall body size index. PC2,
338 accounting for 16% of variance, was positively loaded on bill length but negatively on body
339 mass and tarsus length. Therefore, positive PC1 scores indicated larger nestlings whereas PC2
340 positive scores indicated nestlings with relatively longer bills, lower body mass and shorter tarsi
341 (Table S6). Control nestlings had significantly lower PC1 scores and higher PC2 scores than
342 shaded counterparts (Table 2; Fig. 2). Confirming previous results, T_{nest} was negatively
343 correlated with PC1 and positively with PC2, with T_{nest} being a stronger predictor of morphology
344 than shading treatment (Table S8). PCA also revealed significant sexual dimorphism, with males
345 characterized by smaller size and relatively shorter bills (lower PC1 and PC2 scores; Table 2a,b).
346 While nestling age and year were associated with PC1 and PC2, respectively (Table 2), their
347 interactions with treatment (or T_{nest}) were non-significant.

348

349 *Effect of nestling size and early development on subsequent survival*

350 Age-corrected body mass and tarsus length at hatching were positively correlated with survival
351 in both experimental groups, with no significant interaction between shading and nestling size
352 (Table 3). As expected (Corregidor-Castro et al., 2023), nestlings from shaded nests and higher-
353 ranking nestlings had higher survival (see full models in Table S9). This positive correlation
354 between body size and nestling survival was confirmed using measurements at near-hatching
355 (body mass, tarsus and bill length), again with no significant interaction between the
356 experimental treatment and the morphological traits. On the other hand, no correlations were
357 detected between relative bill size and survival (Table 3; Table S10; Fig. 3). PCA of near-
358 hatching nestling morphology paralleled results from near-fledging: PC1 explained 77% of
359 variance, positively loaded on body mass, tarsus and bill length; PC2 explained 15% of variance,
360 positively loaded on bill length but negatively on tarsus length and body mass (Table S6). As
361 above, positive PC1 and PC2 scores corresponded to larger nestlings and nestling with relatively
362 longer bills, respectively. Models based on PC1 and PC2 scores corroborated linear measurement
363 results: PC1 scores positively correlated with subsequent survival, with no significant treatment
364 group interaction, whereas PC2 scores showed no survival correlation (Table 3; Table S11). This
365 indicates that larger nestlings had a similar survival advantage irrespective of temperature, with
366 no measurable advantage of relatively larger bills. Growth rate, expressed as the increase in body
367 mass and tarsus length from ages 1 to 4 days, was positively correlated with survival,
368 irrespective of the shading treatment (Table 3; Table S12). Consistent with previous analyses,
369 higher-ranking nestlings and those from shaded nests tended to have higher survival.

370

371 **Discussion**

372 While the phenotypic responses of birds to climate warming (Bosco et al., 2023; Ryding et al.,
373 2024; Baldwin et al., 2023; but see Wilcox et al., 2024) match predictions from Bergmann's
374 (body size reduction) and Allen's (relative bill length increase) ecogeographical rules,
375 controversy remains about the proximate and ultimate drivers of such body size and shape shifts
376 (Nord et al., 2024; Youngflesh et al., 2024). Some interpret the shape-shifting as an adaptive
377 process resulting from enhanced survival of smaller birds with relatively longer appendages (e.g.
378 Youngflesh et al., 2024) and/or adaptive developmental plasticity (e.g. Larson et al., 2018).

379 Others suggest observed shape changes largely result from neutral or non-adaptive
380 developmental plasticity (e.g. Siepielski et al., 2019; Nord et al., 2024).

381 Our study is the first to simultaneously investigate, in a field experiment, how nest
382 temperature affects nestling morphological development, and whether the link between nestling
383 morphology and survival changes according to the temperature nestlings experience, providing
384 answers to the above questions. First, we found that near-fledging nestlings from warm,
385 unshaded (control) nest boxes had a smaller body size (lower body mass and shorter tarsus
386 length – see also Corregidor-Castro et al., 2023) and a relatively longer bill, compared to
387 nestlings from the colder, shaded nest boxes. The effect of temperature on nestling morphology
388 was more evident when considering the maximum daily temperatures recorded in the nests
389 during the ten days prior to morphological measurements. This is expected, as although shading
390 significantly reduced the average nest temperature, the wide variation in environmental air
391 temperatures and the asynchrony among nests led to some overlap in temperatures between
392 control and shaded boxes. Second, our survival analyses confirmed that nestlings with larger
393 body size at hatching had a greater probability of surviving until fledging (age 25 days). While
394 control nests experienced significantly higher nestling mortality than shaded nests, the strength
395 of positive selection on body size did not differ between control and shaded broods. In other
396 words, nestlings with smaller body size at hatching showed no measurable survival advantage
397 when subsequently exposed to higher temperatures during development. Third, we found that
398 nestlings with an initially faster growth rate (i.e. larger increase in body size between ages 1 and
399 4 days) had better survival. Again, selection for growth rate did not differ between control and
400 shaded broods, indicating faster-growing nestlings had a survival advantage irrespective of the
401 temperatures experienced during later development. Fourth, nestlings with relatively longer bills
402 at day 4 (when bill length was first measured) did not significantly differ in subsequent survival
403 to fledging compared to those with relatively shorter bills. As above, no differences were found
404 between control and shaded broods, indicating that nestling body shape morphology did not
405 provide measurable thermoregulatory advantages and, indirectly, that the differences in
406 morphology between shaded and control nestlings were due plasticity. Below we discuss how
407 our results can contribute to interpreting the body size and shape shifts observed in bird
408 populations responding to climate warming.

409

410 *Temperature-related developmental plasticity in body size and shape*

411 The magnitude of the temperature-related morphological shift we observed in near-fledging
412 lesser kestrels is comparable to shifts seen in adult birds of several populations exposed to
413 climate warming over recent decades, in both temperate (Ryding et al., 2021; Youngflesh et al.,
414 2022; Bosco et al., 2023; Ryding et al., 2024) and tropical regions (Dubiner and Meiri, 2022;
415 Zimova et al., 2023). For example, Ryding et al. (2024) found in a study of bird skins from 78
416 species collected over the past century that relative bill size increased 1.5% on average (range -
417 20% to +19.5%). In our study, nestlings from the hottest nests (45°C) had 8.4% longer bills
418 relative to body size compared to those from the coldest nests (35°C), corresponding to a $0.8\% \pm$
419 0.4 SE increase in relative bill length per 1°C rise in maximum nest temperature. As summer
420 (June-August) land temperatures in Europe have increased about 2°C in recent decades (Luo et
421 al., 2023), this would correspond to a 1.6% increase in relative bill length - comparable to
422 Ryding et al.'s (2024) findings. Our results indicate body size and shape shifts reported in bird
423 populations may potentially be explained entirely by developmental plasticity.

424 However, the extent to which the temperature effect on fledging morphology will
425 influence adult body size and shape in subsequent generations depends on two assumptions. The
426 first is that the temperature-related developmental plasticity observed in near-fledging
427 morphology permanently affects adult morphology. While we lack direct evidence for our lesser
428 kestrel population, high nestling temperatures have been shown to permanently impact adult
429 morphology in other bird species (Mariette and Buchanan, 2016; Andrew et al., 2017; Shipley et
430 al., 2022; Hope and Angelier, 2024; but see Burness et al., 2013). The second assumption is that
431 reproductive recruitment is unaffected by near-fledging morphology, i.e. smaller lesser kestrel
432 fledglings have equal survival and reproductive success as larger counterparts. This seems
433 unlikely, as larger fledglings usually have higher survival to adulthood (Maness and Anderson
434 2013). Predicting plasticity and selection outcomes is further complicated by selection
435 potentially varying across life stages after fledging, such as migration and reproduction, and
436 differing between sexes (Shipley et al., 2022). An analyses of museum skins and morphometric
437 data from live specimens (Romano et al., 2024) will allow to test our prediction.

438

439

440 *Temperature-related selection on nestling body size and shape*

441 We found a clear survival advantage for nestlings with higher body mass and tarsus length at
442 hatching, an advantage further increased by faster nestling growth rates. In contrast, relative bill
443 length at near-hatching showed no significant association with survival. Similar results were
444 found using PC scores reflecting variation in body size and body shape. Importantly, the strength
445 and direction of phenotypic selection on body size, growth rate, and relative bill length did not
446 differ between shaded and control nests, despite control nestlings experiencing higher
447 temperatures and increased mortality under high nest temperatures (Corregidor-Castro et al.,
448 2023). This result implies that smaller size and relatively longer bills provided no measurable
449 thermoregulatory benefits, or that any thermoregulatory benefit was outweighed by positive
450 selection for larger body size and faster growth. Our results align with meta-analytic evidence
451 from longitudinal bird studies and other endothermic and ectothermic vertebrates, showing
452 consistent selection for larger individuals regardless of temperature, remaining stable over time
453 despite observed body size declines (Siepielski et al., 2019; but see Shipley et al., 2022). We
454 think that our results are important, as we provide experimental evidence that, in free living birds
455 and independently from other ecological factors associated with climatic variation (e.g. Grant
456 and Grant, 1993; Major et al., 2024), high temperatures had no effect on the strength and
457 direction of selection for body size and shape in birds, as predicted by the thermoregulatory
458 hypothesis. This result indirectly concurs with recent laboratory experiments (e.g. Tabh and
459 Nord, 2023; Nord et al., 2024; Tabh et al., 2024) suggesting that thermoregulatory advantage
460 may not be the most relevant explanation for the observed body size and shape shifting observed
461 in bird populations exposed to climate warming. Our results were also in accord with a
462 comparative study of 51 Panamanian bird species which found a temporal decline in body
463 condition in most of these species, concluding nutritional stress, rather than an adaptive warming
464 response, likely caused body size changes (Wilcox et al., 2024).

465

466 *Conclusions*

467 Climate warming is associated with increased frequency and intensity of extreme high
468 temperature events like heatwaves (Rogers et al., 2022; Suarez-Gutierrez et al., 2023). Our
469 results suggest that, particularly in areas where high temperatures occur during the breeding

470 season (e.g. Mediterranean), nestling development can be affected, resulting in reduced body size
471 (mass and tarsus length) and increased relative bill length. We demonstrated that temperature-
472 related developmental plasticity can produce near-fledging morphology matching predictions of
473 Bergmann's (smaller mass and tarsus) and Allen's (longer relative bill) rules. However, we found
474 no evidence that this plasticity may be adaptive, as larger nestlings and those with faster growth
475 had higher survival, while relatively longer bills did not significantly affect pre-fledging survival,
476 regardless of developmental temperatures experienced. While heatwaves during development
477 may affect survival after fledging (Lv et al., 2023) and potentially alter the direction and strength
478 of selection on body morphology, such effects would need to be substantial to counteract the
479 significant impacts temperature had on nestling development and survival observed in our study.
480 This warrants further investigation. In conclusion, despite widespread evidence of shrinking
481 body size and relatively longer appendages in birds and other animals responding to climate
482 warming, our results align with others concluding little empirical support for the idea that
483 thermoregulatory adaptations drive these changes. As we approach critical thresholds in climate
484 warming and extreme temperatures, understanding how temperature affects individual
485 development and survival is essential for predicting climate change effects on population
486 responses and adaptation in birds.

487

488 **Declaration of Interest**

489 None

490

491 **Author contributions**

492 Conceptualization: ACC, AP, DR, JGC; Data collection: ACC, JM, AR, MM; Formal analysis:
493 ACC, AP; Writing - original draft: ACC, AP; Writing - review and editing: all authors
494 contributed to the final draft of the manuscript.

495

496 **Acknowledgments**

497 We are grateful to E. De Capua and E. Eletti for supporting fieldwork in Matera. Nest boxes
498 were built and purchased under the framework of the LIFE Project “Rapaci Lucani”

499 (LIFE05NAT/IT/00009). Monitoring of nest boxes and acquisition of equipment was carried
500 with partial financial support from the LIFE project LIFE FALKON (LIFE17 NAT/IT/000586),
501 from PRIN 2017 (grant number 20178T2PSW to D.R. and A.P.) and PRIN 2022 (grant number
502 2022CWMRNH to A.R., A.P. and M.M.). A.C.-C, M.M. and A.P. were supported by the Italian
503 Ministry of University and Research (project funded by the European Union - Next Generation
504 EU: “PNRR Missione 4 Componente 2, “Dalla ricerca all’impresa”, Investimento 1.4, Progetto
505 CN00000033”). D.R. was also partly supported by Ecosistema MUSA – Multilayered Urban
506 Sustainability Action (funded by the European Union – NextGenerationEU under the NRRP
507 M4C2 Investment Line 1.5: Strengthening of research structures and creation of R&D
508 “innovation ecosystems”, set up of “territorial leaders in R&D”, project ECS_00000037).

509

510 **References**

- 511 Allen, J. A. 1877. The influence of physical conditions in the genesis of species. *Radical Rev.*
512 1:108-140.
- 513 Andrew, S.C., L. L. Hurley, M. M. Mariette, and S. C. Griffith. 2017. Higher temperatures
514 during development reduce body size in the zebra finch in the laboratory and in the wild.
515 *J. Evol. Biol.* 30(12): 2156-2164. <https://doi.org/10.1111/jeb.13181>
- 516 Aparicio, J. M. 1997. Costs and benefits of surplus offspring in the lesser kestrel (*Falco*
517 *naumanni*). *Behav Ecol Sociobiol* 41(2):129-137. <https://doi.org/10.1007/s002650050372>
- 518 Baldwin, J.W., Garcia-Porta, J. and Botero, C.A. 2023. Complementarity in Allen's and
519 Bergmann's rules among birds. *Nat Com* 14: 4240.
520 <https://doi.org/10.1038/s41467-023-39954-9>
- 521 Bates, D., M. Mächler, B. Bolker, and S. Walker. 2015. Fitting Linear Mixed-Effects Models
522 Using lme4. *J. Stat. Softw.* 67(1):1 - 48. <https://doi.org/10.18637/jss.v067.i01>
- 523 Bergmann, C. 1847. Ueber die Verhältnisse der Wärmeökonomie der Thiere zu ihrer Größe.
524 *Göttingen Studien* 3:595-708.
- 525 Bosco, L., A. Otterbeck, T. Fransson, A. Lindén, M. Piha, and A. Lehikoinen. 2023. Increasing
526 winter temperatures explain body size decrease in wintering bird populations of Northern
527 Europe-But response patterns vary along the spatioclimatic gradient. *Glob. Ecol.*
528 *Biogeogr.* <https://doi.org/10.1111/geb.13754>
- 529 Braziotis, S., Liordos, V., Bakaloudis, D.E., Goutner, V., Papakosta, M.A. and Vlachos, C.G.,
530 2017. Patterns of postnatal growth in a small falcon, the lesser kestrel *Falco naumanni*
531 (Fleischer, 1818)(Aves: Falconidae). *Eur. Zool. J.* 84(1): 277-285.
532 <https://doi.org/10.1080/24750263.2017.1329359>
- 533 Brooks, M. E., Kristensen, K., Van Benthem, K. J., Magnusson, A., Berg, C. W., Nielsen, A.,
534 Skaug, H. J., Machler, M., Bolker, B.M. and Bolker, B.M. 2017. glmmTMB balances
535 speed and flexibility among packages for zero-inflated generalized linear mixed
536 modeling. *The R journal*, 9(2), 378-400. <https://doi.org/10.32614/RJ-2017-066>
- 537 Burness, G., J. R. Huard, E. Malcolm, and G. J. Tattersall. 2013. Post-hatch heat warms adult
538 beaks: irreversible physiological plasticity in Japanese quail. *Proc. Royal Soc. B.* 280
539 (1767): 20131436. <https://doi.org/10.1098/rspb.2013.1436>
- 540 Campbell-Tennant, D. J. E., J. L. Gardner, M. R. Kearney, and M. R. E. Symonds. 2015.
541 Climate-related spatial and temporal variation in bill morphology over the past century in
542 Australian parrots. *J. Biogeogr.* 42(6):1163-1175. <https://doi.org/10.1111/jbi.12499>
- 543 Campobello, D., J. Lindstrom, R. Di Maggio, and M. Sara. 2017. An integrated analysis of
544 micro- and macro-habitat features as a tool to detect weather-driven constraints: A case
545 study with cavity nesters. *PLoS one* 12(3). <https://doi.org/10.1371/journal.pone.0174090>
- 546 Cardilini, A. P., K. L. Buchanan, C. D. Sherman, P. Cassey, and M. R. Symonds. 2016. Tests of
547 ecogeographical relationships in a non-native species: what rules avian morphology?
548 *Oecologia* 181(3):783-793. <https://doi.org/10.1007/s00442-016-3590-9>

- 549 Catry, I., T. Catry, P. Patto, A. M. A. Franco, and F. Moreira. 2015. Differential heat tolerance in
550 nestlings suggests sympatric species may face different climate change risks. *Clim. Res.*
551 66(1):13-24. <https://doi.org/10.3354/cr01329>
- 552 Catry, I., A. M. A. Franco, and W. J. Sutherland. 2011. Adapting conservation efforts to face
553 climate change: Modifying nest-site provisioning for lesser kestrels. *Biol Conserv*
554 144(3):1111-1119. <https://doi.org/10.1016/j.biocon.2010.12.030>
- 555 Cerini, F., Childs, D.Z., and Clements, C.F. 2023. A predictive timeline of wildlife population
556 collapse. *Nature Ecology & Evolution*, 7(3), 320-331. [https://doi.org/10.1038/s41559-](https://doi.org/10.1038/s41559-023-01985-2)
557 [023-01985-2](https://doi.org/10.1038/s41559-023-01985-2)
- 558 Corregidor-Castro, A., and Jones, O.R. 2021. The effect of nest temperature on growth and
559 survival in juvenile Great Tits *Parus major*. *Ecol. Evol.* 11(12):7346-7353.
560 <https://doi.org/10.1002/ece3.7565>
- 561 Corregidor-Castro, A., Militti, S., Morinay, J., Romano, A., Morganti, M., Cecere, J.G.,
562 Rubolini, D. and Pilastro, A. 2024. Facing the heat: nestlings of a cavity-nesting raptor
563 trade safety for food when exposed to high nest temperatures, *Anim. Behav.* In press.
564 <https://doi.org/10.1016/j.anbehav.2024.10.020>
- 565 Corregidor-Castro, A., J. Morinay, S. E. McKinlay, S. Ramellini, G. Assandri, G. Bazzi, A.
566 Glavaschi, E. L. De Capua, A. Grapputo, A. Romano, M. Morganti, J. G. Cecere, A.
567 Pilastro, and D. Rubolini. 2023. Experimental nest cooling reveals dramatic effects of
568 heatwaves on reproduction in a Mediterranean bird of prey. *Glob Chang Biol*
569 29(19):5552-5567. <https://doi.org/10.1111/gcb.16888>
- 570 Dubiner, S., and S. Meiri. 2022. Widespread recent changes in morphology of Old World birds,
571 global warming the immediate suspect. *Glob. Ecol. Biogeogr.* 31(4):791-801.
572 <https://doi.org/10.1111/geb.13474>
- 573 Fröhlich, A., D. Kotowska, R. Martyka, and M. R. E. Symonds. 2023. Allometry reveals trade-
574 offs between Bergmann's and Allen's rules, and different avian adaptive strategies for
575 thermoregulation. *Nat Commun* 14(1):1101. [https://doi.org/10.1038/s41467-023-36676-](https://doi.org/10.1038/s41467-023-36676-w)
576 [w](https://doi.org/10.1038/s41467-023-36676-w)
- 577 Gardner, J. L., A. Peters, M. R. Kearney, L. Joseph, and R. Heinsohn. 2011. Declining body size:
578 a third universal response to warming? *Trends Ecol Evol* 26(6):285-291.
579 <https://doi.org/10.1016/j.tree.2011.03.005>
- 580 Gardner, J. L., M. R. Symonds, L. Joseph, K. Ikin, J. Stein, and L. E. Kruuk. 2016. Spatial
581 variation in avian bill size is associated with humidity in summer among Australian
582 passerines. *Clim. Change* 3(1):1-11. <https://doi.org/10.1186/s40665-016-0026-z>
- 583 Grant, B.R. and P.R. Grant. 1993. Evolution of Darwin Finches Caused by A Rare Climatic
584 Event. *Proc. Royal Soc. B.* 251: 111-117. <https://doi.org/10.1098/rspb.1993.0016>
- 585 Grant, P.R., and B.R. Grant. 2008. Pedigrees, assortative mating and speciation in Darwin's
586 finches. *Proc. Royal Soc. B.* 275(1635):661-668. <https://doi.org/10.1098/rspb.2007.0898>

587 Greenberg, R., Cadena, V., Danner, R. M., and Tattersall, G. 2012. Heat loss may explain bill
588 size differences between birds occupying different habitats. PLoS One, 7(7), e40933.
589 <https://doi.org/10.1371/journal.pone.0040933>

590 Hope, S.F., and Angelier, F. 2024. Effects of the temperature during embryonic development on
591 adult reproduction and the phenotype of the second generation in zebra finches. Journal
592 of Thermal Biology, 119, 103787. <https://doi.org/10.1016/j.jtherbio.2024.103787>

593 James, F. C. 1991. Complementary Descriptive and Experimental Studies of Clinal Variation in
594 Birds. Am. Zool. 31(4):694-706. <https://doi.org/10.1093/icb/31.4.694>

595 Jirinec, V., C. Burner Ryan, R. Amaral Bruna, O. Bierregaard Richard, G. Fernández-Arellano,
596 A. Hernández-Palma, I. Johnson Erik, E. Lovejoy Thomas, L. Powell Luke, L. Rutt
597 Cameron, D. Wolfe Jared, and C. Stouffer Philip. 2021. Morphological consequences of
598 climate change for resident birds in intact Amazonian rainforest. Sci. Adv.
599 7(46):eabk1743. <https://doi.org/10.1126/sciadv.abk1743>

600 Krist, M. 2011. Egg size and offspring quality: a meta-analysis in birds. Biol. Rev. 86(3), 692-
601 716. <https://doi.org/10.1111/j.1469-185X.2010.00166.x>

602 La Gioia, G., Melega, L. and Fornasari, L. 2017. Piano d'Azione Nazionale per il grillaio Falco
603 naumanni: Quaderni di Conservazione della Natura 41 MATTM – ISPRA, Roma

604 Larson, E. R., J. R. Eastwood, S. Micallef, J. Wehbe, A. T. D. Bennett, and M. L. Berg. 2018.
605 Nest microclimate predicts bill growth in the Adelaide rosella (Aves: Psittaculidae). Biol
606 J Linn Soc 124(3):339-349. <https://doi.org/10.1093/biolinnean/bly058>

607 Lee, H., K. Calvin, D. Dasgupta, G. Krinner, A. Mukherji, P. Thorne, C. Trisos, J. Romero, P.
608 Aldunce, and K. Barret. 2023. IPCC, 2023: Climate Change 2023: Synthesis Report,
609 Summary for Policymakers. Contribution of Working Groups I, II and III to the Sixth
610 Assessment Report of the Intergovernmental Panel on Climate Change [Core Writing
611 Team, H. Lee and J. Romero (eds.)]. IPCC, Geneva, Switzerland. IPCC, Geneva,
612 Switzerland.

613 Lessells, C. M., and P. T. Boag. 1987. Unrepeatable Repeatabilities: A Common Mistake. The
614 Auk 104(1):116-121. <https://doi.org/10.2307/4087240>

615 Luo, B., Luo, D., Zhuo, W., Xiao, C., Dai, A., Simmonds, I., Yao, Y., Diao, Y. And Gong, T.
616 2023. Increased summer European heatwaves in recent decades: Contributions from
617 greenhouse gases-induced warming and Atlantic Multidecadal Oscillation-like variations.
618 Earth's Future, 11, e2023EF003701. <https://doi.org/10.1029/2023EF003701>

619 Lv, L., M. van de Pol, H. L. Osmond, Y. Liu, A. Cockburn, and L. E. B. Kruuk. 2023. Winter
620 mortality of a passerine bird increases following hotter summers and during winters with
621 higher maximum temperatures. Sci. Adv. 9(1):eabm0197.
622 <https://doi.org/10.1126/sciadv.abm0197>

623 Lüdecke, D., M. S. Ben-Shachar, I. Patil, P. Waggoner, and D. Makowski. 2021. performance:
624 An R package for assessment, comparison and testing of statistical models. J. Open
625 Source Softw. 6(60). <https://doi.org/10.21105/joss.03139>

626 Maness, T.J., and Anderson, D.J. 2013. Predictors of juvenile survival in birds. *Ornithol.*
627 *Monogr.* 78(1), 1-55. <https://www.jstor.org/stable/10.1525/om.2013.78.1.1>

628 Mariette, M. M., and K. L. Buchanan. 2016. Prenatal acoustic communication programs
629 offspring for high posthatching temperatures in a songbird. *Science* 353(6301):812-814.
630 <https://doi.org/10.1126/science.aaf7049>

631 Mayr, E. 1956. Geographical Character Gradients and Climatic Adaptation. *Evolution* 10(1):105-
632 108. <https://doi.org/10.2307/2406103>

633 McQueen, A., Barnaby, R., Symonds, M.R., and Tattersall, G.J. 2023. Birds are better at
634 regulating heat loss through their legs than their bills: implications for body shape
635 evolution in response to climate. *Biology Letters*, 19(11), 20230373.
636 <https://doi.org/10.1098/rsbl.2023.0373>

637 McQueen, A., M. Klaassen, G. J. Tattersall, R. Atkinson, R. Jessop, C. J. Hassell, M. Christie,
638 M. R. E. Symonds, G. Victorian Wader Study, and G. Australasian Wader Studies. 2022.
639 Thermal adaptation best explains Bergmann's and Allen's Rules across ecologically
640 diverse shorebirds. *Nat Commun* 13:4727. <https://doi.org/10.1038/s41467-022-32108-3>

641 Morinay, J., F. De Pascalis, D. M. Dominoni, M. Morganti, F. Pezzo, S. Pirrello, M. Visceglia,
642 E. L. De Capua, J. G. Cecere, and D. Rubolini. 2021. Combining social information use
643 and comfort seeking for nest site selection in a cavity-nesting raptor. *Anim. Behav.*
644 180:167-178. <https://doi.org/10.1016/j.anbehav.2021.07.014>

645 Nakagawa, S., P. C. D. Johnson, and H. Schielzeth. 2017. The coefficient of determination R^2
646 and intra-class correlation coefficient from generalized linear mixed-effects models
647 revisited and expanded. *J. R. Soc. Interface* 14(134): 20170213.
648 <https://doi.org/10.1098/rsif.2017.0213>

649 Nord, A., E. Persson, J. K. R. Tabh, and E. Thoral. 2024. Shrinking body size may not provide
650 meaningful thermoregulatory benefits in a warmer world. *Nat. Ecol. Evol.*
651 <https://doi.org/10.1038/s41559-023-02307-2>

652 Podofillini, S., J. G. Cecere, M. Griggio, M. Corti, E. L. De Capua, M. Parolini, N. Saino, L.
653 Serra, and D. Rubolini. 2019. Benefits of extra food to reproduction depend on maternal
654 condition. *Oikos* 128(7):943-959. <https://doi.org/10.1111/oik.06067>

655 Podofillini, S., J. G. Cecere, M. Griggio, A. Curcio, E. L. De Capua, E. Fulco, S. Pirrello, N.
656 Saino, L. Serra, M. Visceglia, and D. Rubolini. 2018. Home, dirty home: effect of old
657 nest material on nest-site selection and breeding performance in a cavity-nesting raptor.
658 *Curr Zool* 64(6):693-702. <https://doi.org/10.1093/cz/zoy012>

659 Prokosch, J., Z. Bernitz, H. Bernitz, B. Erni, and R. Altwegg. 2019. Are animals shrinking due to
660 climate change? Temperature-mediated selection on body mass in mountain wagtails.
661 *Oecologia* 189(3):841-849. <https://doi.org/10.1007/s00442-019-04368-2>

662 R Core Team. 2024. R: A language and environment for statistical computing. Foundation for
663 Statistical Computing, Vienna, Austria. URL <https://www.R-project.org/>

664 Ramellini, S., S. Imperio, J. Morinay, F. De Pascalis, C. Catoni, M. Morganti, D. Rubolini, and J.
665 G. Cecere. 2022. Individual foraging site fidelity increases from incubation to nestling
666 rearing in a colonial bird. *Anim Behav* 193:145-155.
667 <https://doi.org/10.1016/j.anbehav.2022.07.014>

668 Rogers, C. D. W., K. Kornhuber, S. E. Perkins-Kirkpatrick, P. C. Loikith, and D. Singh. 2022.
669 Sixfold Increase in Historical Northern Hemisphere Concurrent Large Heatwaves Driven
670 by Warming and Changing Atmospheric Circulations. *J. Clim.* 35(3):1063-1078.
671 <https://doi.org/10.1175/JCLI-D-21-0200.1>

672 Romano, A., Corti, M., Soravia, C., Cecere, J. G., and Rubolini, D. 2021. Ectoparasites exposure
673 affects early growth and mouth colour in nestlings of a cavity-nesting raptor. *Behavioral*
674 *Ecology and Sociobiology*, 75, 1-15. <https://doi.org/10.1007/s00265-021-03098-x>

675 Romano, A., Florent, G., Novelli, A., Séchaud, R., and Roulin, A. 2024. Spatio-temporal shift in
676 body size and plumage coloration is associated with the magnitude of climate change in a
677 cosmopolitan owl. *Journal of Biogeography*. <https://doi.org/10.1111/jbi.14863>

678 Ryding, S., M. Klaassen, G. J. Tattersall, J. L. Gardner, and M. R. E. Symonds. 2021. Shape-
679 shifting: changing animal morphologies as a response to climatic warming. *Trends Ecol*
680 *Evol* 36(11): 1036-1048. <https://doi.org/10.1016/j.tree.2021.07.006>

681 Ryding, S., McQueen, A., Klaassen, M., Tattersall, G. J., and Symonds, M. R. E. 2024. Long-
682 and short-term responses to climate change in body and appendage size of diverse
683 Australian birds. *Global Change Biology*, 30, e17517. <https://doi.org/10.1111/gcb.17517>

684 Ryeland, J., Weston, M.A. and Symonds, M.R.E. 2019. Leg length and temperature determine
685 the use of unipedal roosting in birds. *J Avian Biol*, 50: <https://doi.org/10.1111/jav.02008>

686 Salas, R., Lens, L., Stienen, E., Verbruggen, F., and Müller, W. 2022. Growing up in a crowd:
687 social environment shapes the offspring's early exploratory phenotype in a colonial
688 breeding species. *Royal Society Open Science*, 9(10), 220839.
689 <https://doi.org/10.1098/rsos.220839>

690 Santoro, S., and Calzada, J. 2022. Allometry to evaluate Allen's rule in climate warming. *Trends*
691 *Ecol. Evol.* 37(6): 475-477. <https://doi.org/10.1016/j.tree.2022.02.012>

692 Sauve, D., Friesen, V. L., and Charmantier, A. 2021. The effects of weather on avian growth and
693 implications for adaptation to climate change. *Frontiers in Ecology and Evolution*, 9,
694 569741. <https://doi.org/10.3389/fevo.2021.569741>

695 Schneider, C. A., W. S. Rasband, and K. W. Eliceiri. 2012. NIH Image to ImageJ: 25 years of
696 image analysis. *Nat. Methods* 9(7):671-675. <https://doi.org/10.1038/nmeth.2089>

697 Schraft, H.A., Whelan, S., and Elliott, K.H. 2019. Huffin'and puffin: seabirds use large bills to
698 dissipate heat from energetically demanding flight. *J. Exp. Biol.* 222(21), jeb212563.

699 Shipley, J. R., C. W. Twining, C. C. Taff, M. N. Vitousek, and D. W. Winkler. 2022. Selection
700 counteracts developmental plasticity in body-size responses to climate change. *Nat Clim*
701 *Chang.* 12(9):863-868. <https://doi.org/10.1038/s41558-022-01457-8>

702 Siepielski, A. M., Morrissey, M. B., Carlson, S. M., Francis, C. D., Kingsolver, J. G., Whitney,
703 K. D., and Kruuk, L. E. 2019. No evidence that warmer temperatures are associated with

704 selection for smaller body sizes. *Proceedings of the Royal Society B*, 286(1907),
705 20191332.
706 <https://doi.org/10.1098/rspb.2019.1332>

707 Singmann, H., B. Bolker, J. Westfall, F. Aust, and M. Ben-Shachar. 2015. Package ‘afex’.
708 Vienna.

709 Song, S., and Beissinger, S.R. 2020. Environmental determinants of total evaporative water loss
710 in birds at multiple temperatures. *The Auk* 137(1), ukz069.
711 <https://doi.org/10.1093/auk/ukz069>

712 Suarez-Gutierrez, L., W. A. Müller, and J. Marotzke. 2023. Extreme heat and drought typical of
713 an end-of-century climate could occur over Europe soon and repeatedly. *Commun. Earth*
714 *Environ.* 4(1):415. <https://doi.org/10.1038/s43247-023-01075-y>

715 Tabh, J. K. R., and A. Nord. 2023. Temperature-dependent Developmental Plasticity and Its
716 Effects on Allen’s and Bergmann’s Rules in Endotherms. *Integr. Comp. Biol.* 63(3):758-
717 771. <https://doi.org/10.1093/icb/icad026>

718 Tabh, J. K. R., Persson, E., Correia, M., Cuív, C. Ó., Thorald, E., and Nord, A. 2024. No evidence
719 that shrinking and shapeshifting meaningfully affect how birds respond to warming and
720 cooling. *bioRxiv*, 2024.2003.2022.586255. <https://doi.org/10.1101/2024.03.22.586255>

721 Tattersall, G. J., B. Arnaut, and M. R. E. Symonds. 2017. The evolution of the avian bill as a
722 thermoregulatory organ. *Biol Rev Camb Philos Soc* 92(3):1630-1656.
723 <https://doi.org/10.1111/brv.12299>

724 Tian, L., and M. J. Benton. 2020. Predicting biotic responses to future climate warming with
725 classic ecogeographic rules. *Curr Biol* 30(13): R744-R749.
726 <https://doi.org/10.1016/j.cub.2020.06.003>

727 van Gils, J. A., S. Lisovski, T. Lok, W. Meissner, A. Ozarowska, J. de Fouw, E. Rakhimberdiev,
728 M. Y. Soloviev, T. Piersma, and M. Klaassen. 2016. Body shrinkage due to Arctic
729 warming reduces red knot fitness in tropical wintering range. *Science* 352(6287):819-
730 821. <https://doi.org/10.1126/science.aad6351>

731 Weeks, B. C., M. Klemz, H. Wada, R. Darling, T. Dias, B. K. O'Brien, C. M. Probst, M. Zhang,
732 and M. Zimova. 2022. Temperature, size and developmental plasticity in birds. *Biol*
733 *Letters* 18(12):20220357. <https://doi.org/10.1098/rsbl.2022.0357>

734 Weeks, B. C., D. E. Willard, M. Zimova, A. A. Ellis, M. L. Witynski, M. Hennen, and B. M.
735 Winger. 2020. Shared morphological consequences of global warming in North
736 American migratory birds. *Ecol. Lett.* 23(2):316-325. <https://doi.org/10.1111/ele.13434>

737 Wilcox, R. C., Benson, T. J., Brawn, J. D., and Tarwater, C.E. 2024. Observed declines in body
738 size have differential effects on survival and recruitment, but no effect on population
739 growth in tropical birds. *Global Change Biology*, 30(8), e17455.
740 <https://doi.org/10.1111/gcb.17455>

741 Youngflesh, C., J. F. Saracco, R. B. Siegel, and M. W. Tingley. 2022. Abiotic conditions shape
742 spatial and temporal morphological variation in North American birds. *Nat. Ecol. Evol.*
743 6(12):1860-1870. <https://doi.org/10.1038/s41559-022-01893-x>

744 Youngflesh, C., J. F. Saracco, R. B. Siegel, and M. W. Tingley. 2024. Reply to: Shrinking body
745 size may not provide meaningful thermoregulatory benefits in a warmer world. *Nat. Ecol.*
746 *Evol.* <https://doi.org/10.1038/s41559-023-02308-1>
747 Zimova, M., B. C. Weeks, D. E. Willard, S. T. Giery, V. Jirinec, R. C. Burner, and B. M.
748 Winger. 2023. Body size predicts the rate of contemporary morphological change in
749 birds. *Proc. Natl. Acad. Sci.* 120(20):e2206971120.
750 <https://doi.org/10.1073/pnas.2206971120>
751
752
753
754
755
756
757
758
759
760
761
762
763
764
765
766
767
768
769
770
771
772
773
774
775
776
777
778
779
780
781
782
783

784

Tables and Figures

785 **Table 1.** Linear Mixed Models (LMMs) of the effect of the experimental treatment on near-
 786 fledging a) body mass, b) tarsus length and c) bill length ($n = 147$ nestlings, 55 nests). Marginal
 787 R^2 was computed according to Nakagawa et al. (2017) coefficient of determination for LMMs.
 788 Only significant effects are shown; original models, including non-significant predictors, can be
 789 found in the supplementary materials (Table S2).

Predictors	Estimate \pm SE	df	χ^2	p
a) Body mass (g) ($R^2 = 0.20$)				
Treatment (shaded)	7.05 \pm 1.73	1	12.85	< 0.001
Age of the nestling	2.93 \pm 0.77	1	14.10	< 0.001
b) Tarsus length (mm) ($R^2 = 0.33$)				
Treatment (shaded)	0.79 \pm 0.20	1	11.96	< 0.001
Year (2022)	-1.03 \pm 0.27	1	12.08	< 0.001
Age of the nestling	0.20 \pm 0.09	1	4.85	0.03
c) Bill length (mm) ($R^2 = 0.36$)				
Year (2022)	-0.19 \pm 0.06	1	8.00	0.005
Age of the nestling	0.17 \pm 0.03	1	28.95	< 0.001
Sex (male)	-0.19 \pm 0.04	1	19.97	< 0.001

790

791

792

793

794

795 **Table 2.** Linear Mixed Models (LMMs) of the effect of the experimental treatment on nestling
796 body morphology near fledging as described by a Principal Component Analysis of body mass,
797 tarsus and bill length where PC1 represents an index of body size and PC2 and index of body
798 shape ($n = 147$ nestlings, 55 nests). Positive PC1 scores represent larger nestlings, whereas
799 positive PC2 scores represent nestlings with relatively longer bills (more details on the PCA are
800 given on Table S6). Marginal R^2 was computed according to Nakagawa et al. (2017) coefficient
801 of determination for LMMs. Only significant effects are shown; original models, including non-
802 significant predictors, can be found in the supplementary materials (Table S7).

Predictors	Estimate \pm SE	df	χ^2	p
a) PC1 (body size index) ($R^2 = 0.34$)				
Treatment (shaded)	0.51 \pm 0.13	1	11.93	<0.001
Year (2022)	-1.11 \pm 0.38	1	7.52	0.006
Age of the nestling	0.28 \pm 0.07	1	17.46	<0.001
Sex (male)	-0.20 \pm 0.08	1	6.48	0.01
b) PC2 (body shape index) ($R^2 = 0.17$)				
Treatment (shaded)	-0.14 \pm 0.07	1	4.66	0.04
Age of the nestling	0.12 \pm 0.03	1	11.70	<0.001
Sex (male)	-0.19 \pm 0.05	1	15.21	<0.001

803

804

805

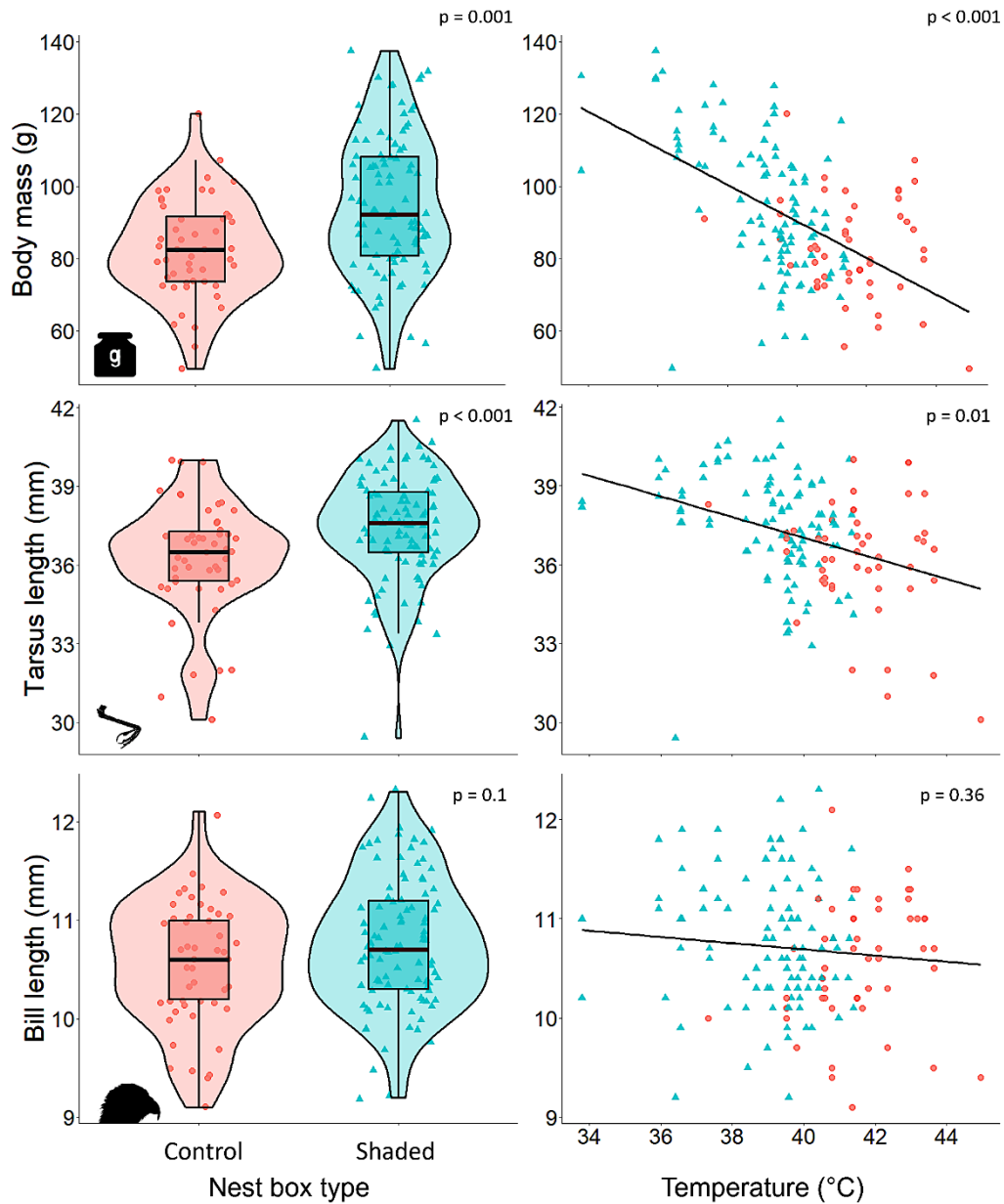
806

807

808

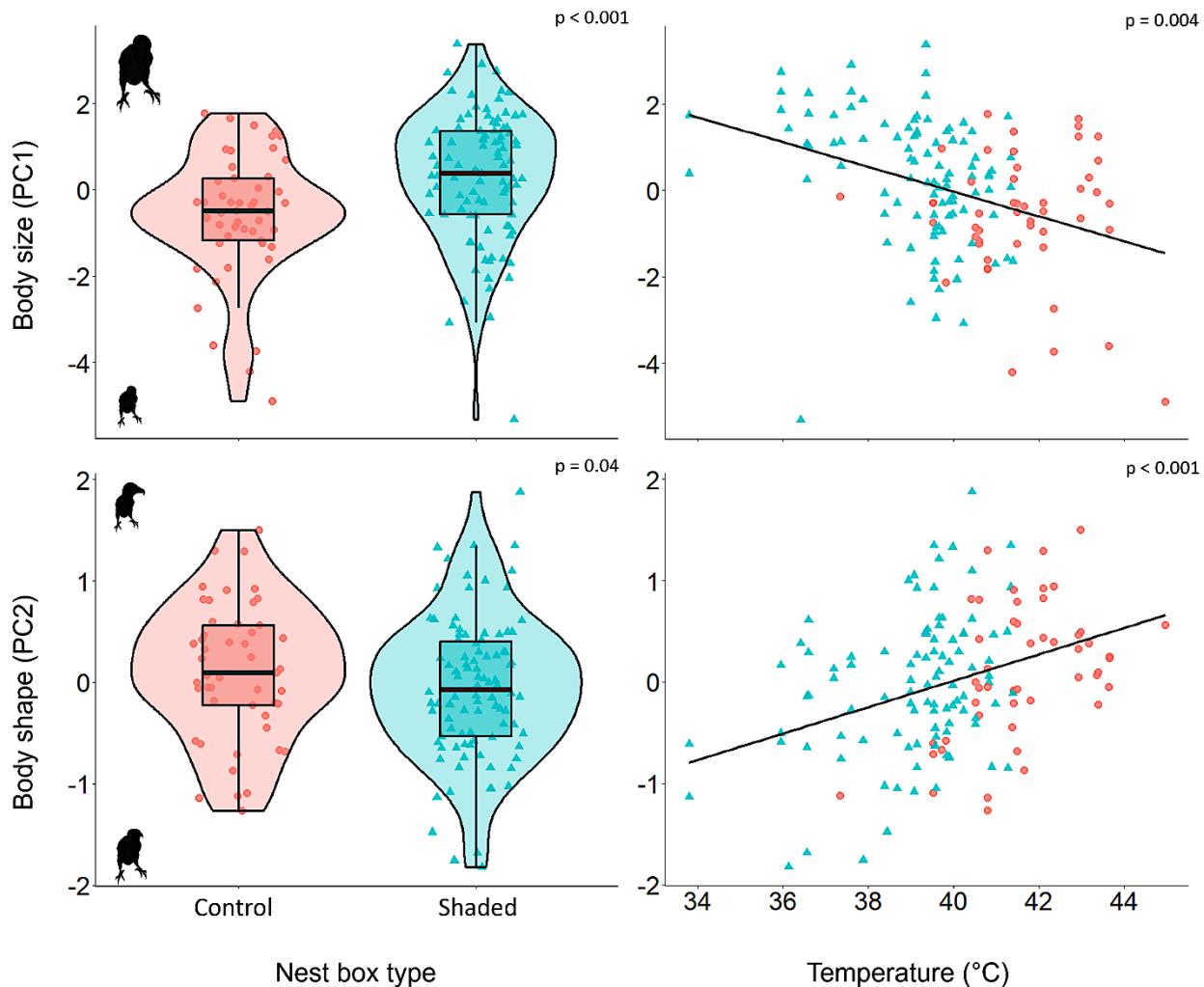
809 **Table 3.** Association between nestling morphology at hatching (age 1 day) and near hatching
810 (age 4 days) and subsequent survival to fledging (age 25 days) in relation to the experimental
811 treatment. As for morphology near fledging, we used measurement of body morphology (age
812 corrected body mass, tarsus length and bill length) and their linear combination using a PCA
813 (positive PC1 scores represented larger nestlings and positive PC2 scores represented nestlings
814 with relatively longer bills, see Table S6 for further details). Furthermore, we calculated the
815 association between initial nestling body mass and tarsus length growth rate (from age 1 to 4
816 days) and survival. Coefficients and standard errors for the association between morphological
817 traits, experimental treatment (shading), and their interaction were obtained from Generalized
818 Linear Mixed Models (GLMMs) where survival was entered as binomial dependent variable.
819 Full models are presented in the supplementary material (Table S9-12). Significance effects are
820 indicated by asterisks (* = $p < 0.05$; ** = $p < 0.01$; *** = $p < 0.001$).

Nestling morphology		Treatment (shaded)	Morphology × treatment	
Age 1	Body mass (g)	1.14 ± 0.60 *	3.75 ± 1.98 ***	-0.26 ± 0.43
	Tarsus length (mm)	0.93 ± 0.42 *	2.59 ± 0.94 ***	-0.22 ± 0.35
Age 4	Body mass (g)	4.58 ± 1.26 ***	6.79 ± 6.23 ***	1.18 ± 0.61
	Tarsus length (mm)	2.51 ± 0.84 ***	4.23 ± 1.73 ***	0.98 ± 0.64
	Bill length (mm)	1.25 ± 0.75 *	4.78 ± 3.15 ***	0.73 ± 0.47
	Relative bill length (mm)	0.32 ± 0.49	4.19 ± 2.39 ***	0.26 ± 0.37
PCA (age 4)	PC1 ^a (body size index)	4.42 ± 1.41 ***	15.17 ± 5.04 ***	2.21 ± 1.89
	PC2 ^b (body shape index)	-1.06 ± 0.63	5.19 ± 2.27 ***	0.39 ± 0.59
Nestling growth rate (from age 1 to 4)	Body mass growth rate (g/day)	0.83 ± 0.28 ***	2.51 ± 0.98 ***	-0.14 ± 0.22
	Tarsus length growth rate (mm/day)	2.91 ± 1.16 **	3.42 ± 2.18 ***	-0.42 ± 1.00



822

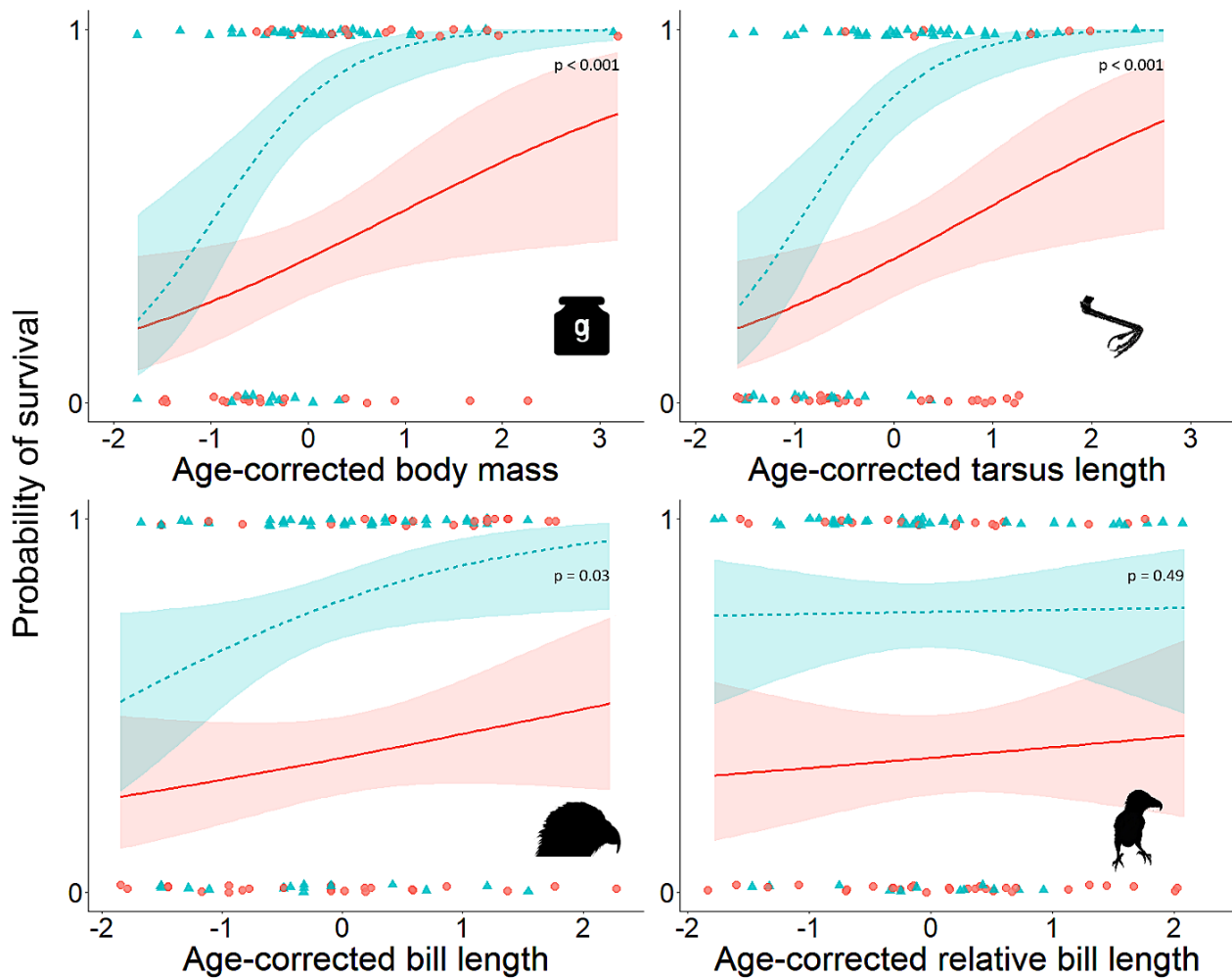
823 **Figure 1.** Body mass (g), tarsus length (mm) and bill length (mm) of control (red, circles) and
 824 shaded (blue, triangles) lesser kestrel nestlings measured near fledging (age 15.6 ± 1.7 days).
 825 Fitted lines were derived from the corresponding LMMs reported in Table S3.



827

828 **Figure 2.** PCA scores representing body size (PC1) and body shape (PC2) in control (red,
 829 circles) and shaded (blue, triangles) lesser kestrel nestlings measured near fledging (age $15.6 \pm$
 830 1.7 days). PC1 was positively loaded to body mass, tarsus length and bill length, and positive
 831 scores therefore represent larger nestlings. PC2 was positively loaded to bill length, and
 832 negatively to body mass and tarsus length, and positive scores therefore represent nestlings with
 833 relatively longer bill (loading factors in Table S6). Fitted lines were derived from the
 834 corresponding LMMs reported in Table S8.

835



837

838 **Figure 3.** Association between body mass, tarsus length, bill length and relative bill length at
 839 near-hatching on subsequent survival in the two experimental treatments (control: red circles and
 840 solid line; shaded: blue triangles and dashed line). Morphological measurements were
 841 standardized for nestling age (age interval: 3-5 days). Relative bill length was calculated as the
 842 residual of the regression of bill length on body mass and tarsus length. Fitted lines (with 95%
 843 confidence bands) were derived from the corresponding GLMMs reported in Table S10. None of
 844 the interactions between the morphological trait and the experimental treatment were significant.

845

846

847

Supplementary Material

848 **Supplementary Tables**

849 **Table S1.** Brood size, nestling age and nestling morphology at hatching (age 0-2 days) and near-
 850 hatching (age 3-5, when bill size was measured for the first time), in the two experimental
 851 treatments (control and shaded nest boxes). Means were estimated from LMMs in which
 852 experimental treatment was entered as fixed factors and nest and dyad identity were entered as
 853 random factors.

	Control nest	Shaded nest	χ^2	
	boxes	boxes		
a) Age 1 day (range 0-2)				854
Body mass (g)	14.3 ± 0.5	13.8 ± 0.5	0.41	855
Tarsus length (mm)	15.1 ± 0.2	15.0 ± 0.2	0.45	856
Mean age of the nestling (days)	0.9 ± 0.1	1.0 ± 0.1	0.08	857
Brood size (number of nestlings)	3.4 ± 0.1	3.6 ± 0.1	2.40	858
				859
b) Age 4 days (range 3-5)				860
Body mass (g)	29.8 ± 1.3	30.2 ± 1.3	0.11	861
Tarsus length (mm)	20.2 ± 0.4	20.3 ± 0.4	0.01	862
Bill length (mm)	7.5 ± 0.9	7.4 ± 0.8	0.79	863
Relative bill length	0.04 ± 0.1	-0.12 ± 0.1	0.78	864
Growth rate body mass (g/day)	4.4 ± 0.3	4.9 ± 0.2	2.07	865
Growth rate tarsus length (mm/day)	1.5 ± 0.1	1.6 ± 0.1	2.56	866
Mean age of the nestling (days)	4.24 ± 0.1	4.21 ± 0.1	0.08	867
Survival (from age 1 to age 4) ^a	0.89 ± 0.1	0.95 ± 0.1	0.61	868

870

871 *Note:* ^aGLMM with binomial error distribution

872 **Table S2.** Linear Mixed Models (LMMs) of the effect of the experimental treatment on near-
873 fledging a) body mass, b) tarsus length and c) bill length ($n = 147$ nestlings, 55 nests). Marginal
874 R^2 was computed according to Nakagawa et al. (2017) coefficient of determination for LMMs.
875 Models include all fixed predictors; all interactions between treatment and the other fixed
876 predictors were non-significant and were excluded from the models.

Predictors	Estimate \pm SE	df	χ^2	p
a) Body mass (g) ($R^2 = 0.23$)				
Treatment (shaded)	6.60 \pm 1.83	1	13.04	0.001
Year (2022)	3.57 \pm 2.61	1	1.88	0.18
Age of the nestling	3.18 \pm 0.78	1	16.74	< 0.001
Hatching rank	-1.29 \pm 2.54	1	0.26	0.61
Sex (male)	-1.57 \pm 0.91	1	2.97	0.09
Brood size	-2.02 \pm 1.99	1	1.02	0.32
b) Tarsus length (mm) ($R^2 = 0.35$)				
Treatment (shaded)	0.75 \pm 0.20	1	13.88	< 0.001
Year (2022)	-1.18 \pm 0.28	1	17.48	< 0.001
Age of the nestling	0.23 \pm 0.09	1	6.08	0.02
Hatching rank	-0.40 \pm 0.28	1	2.08	0.16
Sex (male)	-0.06 \pm 0.11	1	0.26	0.61
Brood size	-0.23 \pm 0.22	1	1.13	0.29
c) Bill length (mm) ($R^2 = 0.39$)				
Treatment (shaded)	0.08 \pm 0.05	1	2.99	0.10
Year (2022)	-0.22 \pm 0.07	1	10.15	0.003
Age of the nestling	0.17 \pm 0.03	1	32.31	< 0.001
Hatching rank	-0.11 \pm 0.07	1	2.73	0.11
Sex (male)	-0.17 \pm 0.04	1	17.50	< 0.001
Brood size	0.01 \pm 0.06	1	0.01	0.93

877 **Table S3.** Linear Mixed Models (LMMs) of the effect of T_{nest} on near-fledging a) body mass, b)
878 tarsus length and c) bill length ($n = 147$ nestlings, 55 nests). Marginal R^2 was computed
879 according to Nakagawa et al. (2017) coefficient of determination for LMMs. Models include all
880 fixed predictors; all interactions between treatment and the other fixed predictors were non-
881 significant and were excluded from the models.

Predictors	Estimate \pm SE	df	χ^2	p
a) Body mass (g) ($R^2 = 0.30$)				
T_{nest}	-3.70 ± 0.68	1	20.46	< 0.001
Year (2022)	-3.24 ± 2.12	1	2.28	0.13
Age of the nestling	3.24 ± 0.75	1	17.58	< 0.001
Hatching rank	-2.36 ± 2.11	1	1.23	0.27
Sex (male)	-1.87 ± 0.91	1	4.14	0.04
Brood size	-1.72 ± 1.68	1	0.98	0.32
b) Tarsus length (mm) ($R^2 = 0.35$)				
T_{nest}	-0.26 ± 0.08	1	6.61	0.01
Year (2022)	-1.18 ± 0.25	1	18.13	< 0.001
Age of the nestling	0.24 ± 0.09	1	6.78	0.01
Hatching rank	-0.51 ± 0.25	1	3.87	0.05
Sex (male)	-0.09 ± 0.11	1	0.68	0.41
Brood size	-0.20 ± 0.20	1	0.94	0.33
c) Bill length (mm) ($R^2 = 0.40$)				
T_{nest}	-0.02 ± 0.02	1	0.83	0.36
Year (2022)	-0.22 ± 0.06	1	10.43	0.001
Age of the nestling	0.17 ± 0.03	1	31.37	< 0.001
Hatching rank	-0.12 ± 0.07	1	3.55	0.06
Sex (male)	-0.18 ± 0.04	1	17.92	< 0.001
Brood size	0.01 ± 0.05	1	0.00	0.97

882 **Table S4.** Linear Mixed Models (LMMs) of the effect of the experimental treatment and T_{nest} on
 883 near-fledging bill size relative to body mass and tarsus length ($n = 147$ nestlings, 55 nests).
 884 Marginal R^2 was computed according to Nakagawa et al. (2017) coefficient of determination for
 885 LMMs. Models include all fixed predictors; all interactions between treatment and the other
 886 fixed predictors were non-significant and were excluded from the models.

887

Predictors	Estimate \pm SE	df	χ^2	p
a) Relative bill length – Experimental treatment ($R^2 = 0.55$)				
Body mass	0.01 \pm 0.01	1	1.86	0.17
Tarsus length	0.11 \pm 0.03	1	10.02	0.002
Treatment (shaded)	-0.03 \pm 0.05	1	0.39	0.54
Age of the nestling	0.13 \pm 0.03	1	23.58	< 0.001
Sex (male)	-0.15 \pm 0.04	1	17.11	< 0.001
Hatching rank	-0.06 \pm 0.06	1	1.09	0.30
Year (2022)	-0.17 \pm 0.12	1	1.96	0.16
b) Relative bill length – Nest temperature (T_{nest}) ($R^2 = 0.57$)				
Body mass	0.01 \pm 0.01	1	4.32	0.04
Tarsus length	0.10 \pm 0.03	1	8.68	0.003
T_{nest}	0.05 \pm 0.02	1	4.68	0.03
Age of the nestling	0.12 \pm 0.03	1	20.02	< 0.001
Sex (male)	-0.15 \pm 0.04	1	116.43	< 0.001
Hatching rank	-0.06 \pm 0.06	1	0.99	0.32
Year (2022)	-0.18 \pm 0.12	1	2.29	0.13

888

889

890

891

892 **Table S5.** Linear Mixed Models (LMMs) of the effect of the experimental treatment and T_{nest} on
 893 near-fledging tarsus size relative to body mass ($n = 147$ nestlings, 55 nests). Marginal R^2 was
 894 computed according to Nakagawa et al. (2017) coefficient of determination for LMMs. Models
 895 include all fixed predictors; all interactions between treatment and the other fixed predictors
 896 were non-significant and were excluded from the models.

897

Predictors	Estimate \pm SE	df	χ^2	p
a) Relative tarsus length – Experimental treatment ($R^2 = 0.55$)				
Body mass	0.09 \pm 0.01	1	109.98	<0.001
Treatment (shaded)	-0.14 \pm 0.13	1	1.09	0.30
Age of the nestling	0.04 \pm 0.06	1	0.38	0.54
Sex (male)	-0.07 \pm 0.08	1	0.71	0.40
Hatching rank	-0.30 \pm 0.15	1	3.74	0.05
Year (2022)	-1.72 \pm 0.27	1	27.60	<0.001
b) Relative tarsus length – Nest temperature (T_{nest}) ($R^2 = 0.83$)				
Body mass	0.09 \pm 0.07	1	115.31	<0.001
T_{nest}	0.08 \pm 0.06	1	1.48	0.22
Age of the nestling	0.06 \pm 0.06	1	0.80	0.37
Sex (male)	-0.07 \pm 0.08	1	0.76	0.38
Hatching rank	-0.31 \pm 0.15	1	4.03	0.05
Year (2022)	-1.74 \pm 0.27	1	29.64	<0.001

898

899

900

901

902

903 **Table S6.** Factor loading and proportion of variance explained from PC1 (body size) and PC2
 904 (body shape) axis regarding the morphological data (body mass, tarsus and bill length) of
 905 nestlings at near-hatching (age 4 days; n = 171 nestlings, 73 nests) and at near-fledging (age 15
 906 days; n = 147 nestlings, 55 nests).

907

908

909

910

911

912

913

914

915

916

917

918

919

920

	PC1 ^a (Body size)	PC2 ^b (Body shape)
a) Near hatching (age ± 4 days)		
Body mass	0.59	-0.45
Tarsus length	0.61	-0.30
Bill length	0.53	0.84
Proportion of variance explained	0.77	0.15
b) Near fledging (age ± 15 days)		
Body mass	0.92	-0.27
Tarsus length	0.93	-0.24
Bill length	0.80	0.60
Proportion of variance explained	0.78	0.16

921 *Note:* ^apositive PC1 scores represent larger nestlings; ^bpositive PC2 scores represent nestlings
 922 with relatively longer bills.

923

924

925

926

927

928 **Table S7.** Linear Mixed Models (LMMs) of the effect of the experimental treatment on near-
 929 fledging nestling body morphology as described by a PCA on body mass, tarsus length and bill
 930 length where PC1 represents an index of body size and PC2 a size-corrected index of body shape
 931 ($n = 147$ nestlings, 55 nests). Positive PC1 scores represent larger nestlings, whereas positive
 932 PC2 scores represent nestlings with relatively longer bills (more details on the PCA are given on
 933 Table S6). Marginal R^2 was computed according to Nakagawa et al. (2017) coefficient of
 934 determination for LMMs. Models include all fixed predictors; all interactions between treatment
 935 and the other fixed predictors were non-significant and were excluded from the models.
 936

Predictors	Estimate \pm SE	df	χ^2	p
a) PC1 (body size index) ($R^2 = 0.35$)				
Treatment (shaded)	0.49 \pm 0.13	1	13.72	0.001
Year (2022)	-1.31 \pm 0.40	1	10.64	0.002
Age of the nestling	0.30 \pm 0.07	1	20.10	<0.001
Hatching rank	-0.27 \pm 0.19	1	2.01	0.16
Sex (male)	-0.20 \pm 0.08	1	6.37	0.01
Brood size	-0.12 \pm 0.15	1	0.64	0.42
b) PC2 (body shape index) ($R^2 = 0.19$)				
Treatment (shaded)	-0.16 \pm 0.07	1	4.48	0.04
Year (2022)	-0.06 \pm 0.16	1	0.15	0.70
Age of the nestling	0.11 \pm 0.04	1	10.27	0.002
Hatching rank	-0.07 \pm 0.09	1	0.65	0.42
Sex (male)	-0.18 \pm 0.05	1	14.70	<0.001
Brood size	0.11 \pm 0.07	1	2.07	0.16

937

938

939 **Table S8.** Linear Mixed Models (LMMs) of the effect of T_{nest} on near-fledging nestling body
 940 morphology as described by a PCA on body mass, tarsus length and bill length where PC1
 941 represents an index of body size and PC2 a size-corrected index of body shape ($n = 147$
 942 nestlings, 55 nests). Positive PC1 scores represent larger nestlings, whereas positive PC2 scores
 943 represent nestlings with relatively longer bills (more details on the PCA are given on Table S6).
 944 Marginal R^2 was computed according to Nakagawa et al. (2017) coefficient of determination for
 945 LMMs. Models include all fixed predictors; all interactions between treatment and the other
 946 fixed predictors were non-significant and were excluded from the models.

947

Predictors	Estimate \pm SE	df	χ^2	p
a) PC1 (body size index) ($R^2 = 0.37$)				
T_{nest}	-0.20 \pm 0.06	1	8.22	0.004
Year (2022)	-1.30 \pm 0.35	1	11.92	<0.001
Age of the nestling	0.31 \pm 0.07	1	20.59	<0.001
Hatching rank	-0.34 \pm 0.17	1	3.80	0.05
Sex (male)	-0.23 \pm 0.08	1	7.72	0.01
Brood size	-0.11 \pm 0.14	1	0.59	0.44
b) PC2 (body shape index) ($R^2 = 0.28$)				
T_{nest}	0.13 \pm 0.03	1	16.82	<0.001
Year (2022)	-0.11 \pm 0.14	1	0.60	0.44
Age of the nestling	0.11 \pm 0.03	1	10.65	0.001
Hatching rank	-0.07 \pm 0.08	1	0.69	0.41
Sex (male)	-0.17 \pm 0.05	1	12.60	<0.001
Brood size	0.11 \pm 0.06	1	2.66	0.10

948

949

950

951 **Table S9.** Generalized Linear Mixed Models (GLMMs) of the association between nestling
 952 morphology (body mass and tarsus length) at hatching (age 1 day) and subsequent survival to
 953 fledging (age 25 days) in relation to the experimental treatment. Body mass and tarsus length
 954 were standardized for age differences (age range: 0-2 days). Marginal R^2 was computed
 955 according to Nakagawa et al. (2017) coefficient of determination for GLMMs. Models include
 956 all fixed predictors; all interactions between treatment and the other fixed predictors were non-
 957 significant and were excluded from the models, with the exception of the interaction with
 958 survival, that was maintained in the models.

959

Predictors	Estimate \pm SE	df	χ^2	p
a) Effect of body mass on survival ($R^2 = 0.35$; n = 185 nestlings, 73 nests)				
Body mass (age-corrected)	1.14 \pm 0.60	1	7.58	0.02
Treatment (shaded)	3.75 \pm 1.98	1	23.51	< 0.001
Sex (male)	-0.57 \pm 0.77	1	0.55	0.46
Hatching rank	-1.45 \pm 0.54	1	15.89	< 0.001
Brood size	-0.46 \pm 0.82	1	0.31	0.58
Body mass (age-corrected) \times Treatment (shaded)	-0.26 \pm 0.43	1	0.02	0.90
b) Effect of tarsus length on survival ($R^2 = 0.34$; n = 196 nestlings, 76 nests)				
Tarsus length (age-corrected)	0.93 \pm 0.42	1	6.32	0.01
Treatment (shaded)	2.59 \pm 0.94	1	23.13	< 0.001
Sex (male)	-0.83 \pm 0.90	1	0.91	0.34
Hatching rank	-1.44 \pm 0.42	1	24.48	< 0.001
Brood size	0.15 \pm 0.99	1	0.02	0.88
Tarsus length (age-corrected) \times Treatment (shaded)	-0.22 \pm 0.35	1	0.41	0.52

960

961

962

963 **Table S10.** Generalized Linear Mixed Models (GLMMs) of the association between nestling
 964 morphology (body mass and tarsus length) near hatching (age 4 days) and subsequent survival to
 965 fledging (age 25 days) in relation to the experimental treatment. Body mass, tarsus, bill and
 966 relative bill length were standardized for age differences (age range: 3-5 days). Marginal R^2 was
 967 computed according to Nakagawa et al. (2017) coefficient of determination for GLMMs. Models
 968 include all fixed predictors; all interactions between treatment and the other fixed predictors
 969 were non-significant and were excluded from the models, with the exception of the interaction
 970 with survival, that was maintained in the models.

Predictors	Estimate \pm SE	df	χ^2	p
a) Effect of body mass on survival ($R^2 = 0.40$; n = 182 nestlings, 74 nests)				
Body mass (age-corrected)	4.58 \pm 1.26	1	27.63	< 0.001
Treatment (shaded)	6.79 \pm 6.23	1	30.50	< 0.001
Sex (male)	0.21 \pm 1.20	1	0.04	0.84
Hatching rank	-1.35 \pm 0.78	1	6.87	0.009
Brood size	-1.16 \pm 1.61	1	0.74	0.39
Body mass (age-corrected) \times Treatment (shaded)	1.18 \pm 0.61	1	3.03	0.08
b) Effect of tarsus length on survival ($R^2 = 0.45$; n = 182 nestlings, 74 nests)				
Tarsus length (age-corrected)	2.51 \pm 0.84	1	19.34	< 0.001
Treatment (shaded)	4.23 \pm 1.73	1	26.38	< 0.001
Sex (male)	-0.10 \pm 0.89	1	0.03	0.87
Hatching rank	-1.36 \pm 0.56	1	11.74	< 0.001
Brood size	-1.34 \pm 0.99	1	1.13	0.29
Tarsus length (age-corrected) \times Treatment (shaded)	0.98 \pm 0.64	1	0.63	0.43
c) Effect of bill length on survival ($R^2 = 0.38$; n = 179 nestlings, 73 nests)				
Bill length (age-corrected)	1.25 \pm 0.75	1	5.00	0.03
Treatment (shaded)	4.78 \pm 3.15	1	26.48	< 0.001
Sex (male)	-0.40 \pm 0.87	1	0.22	0.64
Hatching rank	-1.45 \pm 0.67	1	12.98	< 0.001

Brood size	-0.50 ± 1.09	1	0.21	0.65
Bill length (age-corrected) × Treatment (shaded)	0.73 ± 0.47	1	1.80	0.18

d) Effect of relative bill length on survival ($R^2 = 0.34$; n = 179 nestlings, 73 nests)

Bill length (age-corrected)	0.32 ± 0.49	1	0.48	0.49
Treatment (shaded)	4.19 ± 2.39	1	24.72	< 0.001
Sex (male)	-0.91 ± 0.85	1	1.32	0.25
Hatching rank	-1.11 ± 0.48	1	9.44	0.002
Brood size	-0.40 ± 0.91	1	0.20	0.65
Bill length (age-corrected) × Treatment (shaded)	0.26 ± 0.37	1	3.60	0.48

971

972

973

974

975

976

977

978

979

980

981

982

983

984

985

986

987

988

989

990

991 **Table S11.** Generalized Linear Mixed Models (GLMMs) of the effect of the experimental
 992 treatment on near-hatching nestling body morphology as described by a PCA on body mass,
 993 tarsus length and bill length at near hatching (age 4 days; $n = 171$ nestlings, 73 nests) on
 994 subsequent survival to fledging (age 25 days). PC1 represents an index of body size and PC2 a
 995 size-corrected index of body shape. Positive PC1 scores represent larger nestlings, whereas
 996 positive PC2 scores represent nestlings with relatively longer bills (more details on the PCA are
 997 given on Table S6). Marginal R^2 was computed according to Nakagawa et al. (2017) coefficient
 998 of determination for GLMMs. Models include all fixed predictors; all interactions between
 999 treatment and the other fixed predictors were non-significant and were excluded from the
 1000 models.

Predictors	Estimate \pm SE	df	χ^2	p
a) PC1 (body size index) ($R^2 = 0.37$)				
PC1	4.42 \pm 1.41	1	22.90	< 0.001
Treatment (shaded)	15.17 \pm 5.04	1	31.97	< 0.001
Sex (male)	0.61 \pm 1.29	1	0.16	0.69
Hatching rank	-2.00 \pm 0.76	1	12.18	< 0.001
Brood size	-0.86 \pm 1.34	1	1.71	0.19
PC1 \times Shading	2.21 \pm 1.89	1	1.24	0.27
b) PC2 (body shape index) ($R^2 = 0.31$)				
PC2	-1.06 \pm 0.63	1	1.49	0.22
Treatment (shaded)	5.19 \pm 2.27	1	25.44	< 0.001
Sex (male)	-1.22 \pm 0.96	1	1.88	0.17
Hatching rank	-1.18 \pm 0.49	1	8.48	0.004
Brood size	-0.40 \pm 1.05	1	0.13	0.72
PC2 \times Shading	0.39 \pm 0.59	1	0.55	0.46

1001

1002

1003 **Table S12.** Generalized Linear Mixed Models (GLMMs) of the effect of growth rate, i.e. body
1004 mass (g/day) and tarsus length (mm/day) from age 1 to age 4 days ($n = 180$ nestlings, 73 nests)
1005 on subsequent survival to fledging (age 25 days). Marginal R^2 was computed according to
1006 Nakagawa et al. (2017) coefficient of determination for GLMMs. Models include all fixed
1007 predictors; all interactions between treatment and the other fixed predictors were non-significant
1008 and were excluded from the models.

1009

Predictors	Estimate \pm SE	df	χ^2	p
a) Effect of body mass growth rate on survival ($R^2 = 0.39$)				
Growth rate (body mass)	0.83 \pm 0.28	1	13.79	< 0.001
Treatment (shaded)	2.51 \pm 0.98	1	19.59	< 0.001
Sex (male)	-0.45 \pm 0.76	1	0.73	0.39
Hatching rank	-0.75 \pm 0.37	1	3.68	0.06
Brood size	-0.51 \pm 0.67	1	0.62	0.43
Growth rate (body mass) \times Treatment (shaded)	-0.14 \pm 0.22	1	0.23	0.63
b) Effect of tarsus length growth rate on survival ($R^2 = 0.35$)				
Growth rate (tarsus length)	2.91 \pm 1.16	1	9.24	0.002
Treatment (shaded)	3.42 \pm 2.18	1	18.43	< 0.001
Sex (male)	-0.91 \pm 0.89	1	1.21	0.27
Hatching rank	-1.06 \pm 0.49	1	7.87	0.01
Brood size	-0.77 \pm 0.96	1	0.76	0.38
Growth rate (tarsus length) \times Treatment (shaded)	-0.42 \pm 1.00	1	0.17	0.68

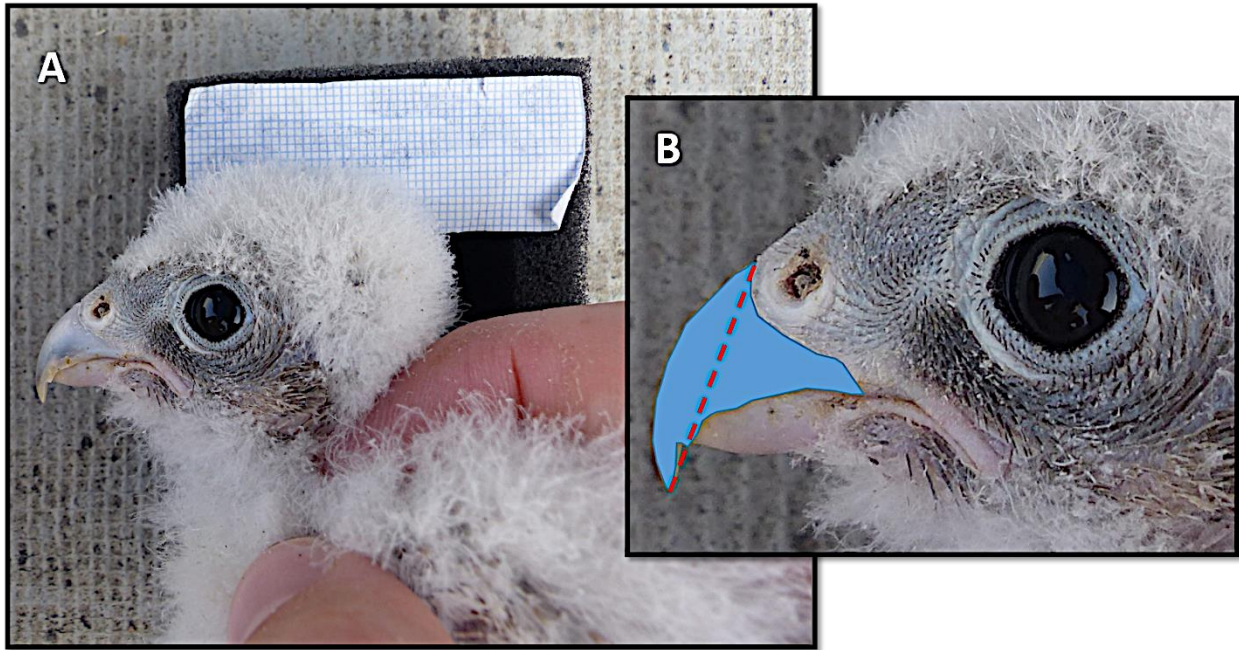
1010

1011

1012

1013 **Supplementary Figures**

1014



1015

1016 **Figure S1.** A) Lateral picture of a nestling on a scaled background. B) Measurement of lateral
1017 bill area (blue), obtained in ImageJ, and bill length (cere to bill tip, measured in the field; red
1018 dashed line).

1019

1020

1021

1022

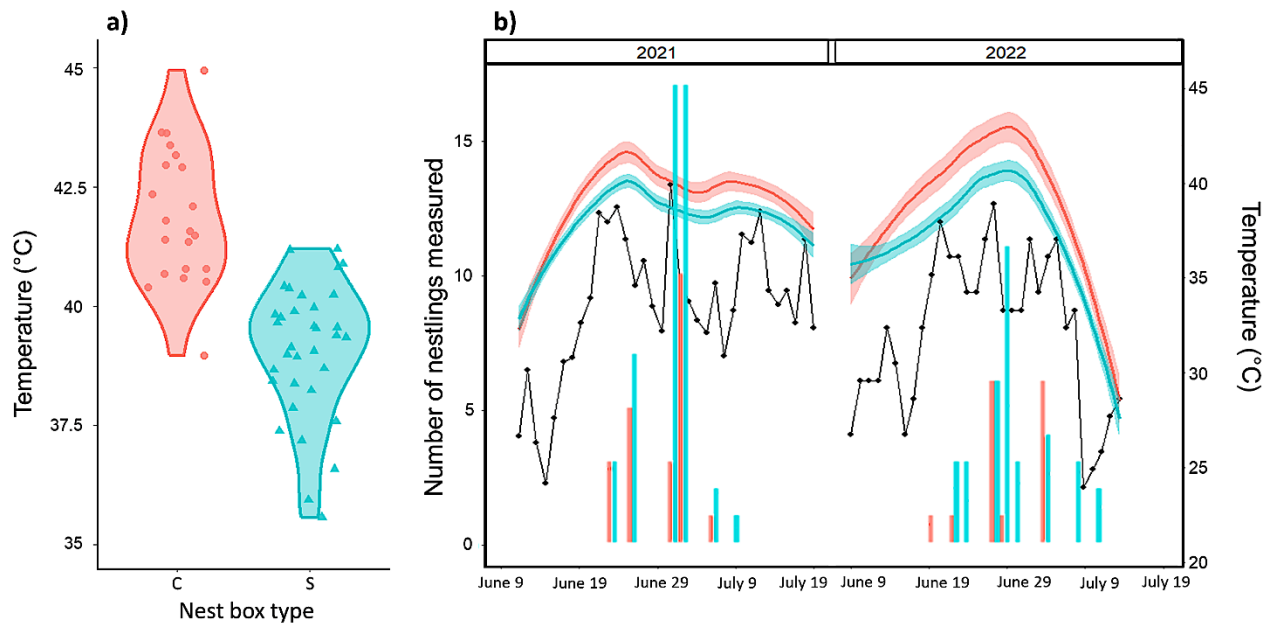
1023

1024

1025

1026

1027



1029

1030 **Figure S2.** A) T_{nest} (average of daily maximum temperatures) in control (red circles) and shaded
 1031 (blue triangles) nest boxes during the 10 days before the last biometric measurements were taken
 1032 on lesser kestrel nestlings. B) Daily maximum air temperature (black dots and line) recorded in
 1033 the study area during the experiment (data from Matera city weather station,
 1034 <https://centrofunzionale.regione.basilicata.it/>) and daily mean maximum nest temperature in
 1035 control (red line) and shaded (blue line) nest boxes. Vertical bars represent the number of
 1036 nestlings measured per day during the last visit (red: control nestlings; blue: shaded nestlings).

1037

1038